DE GRUYTER Rev Chem Eng 2022; 38(3): 273–299

Review

Rouzbeh Ramezani*, Saeed Mazinani and Renzo Di Felice

State-of-the-art of CO_2 capture with amino acid salt solutions

https://doi.org/10.1515/revce-2020-0012
Received February 18, 2020; accepted June 24, 2020;

Abstract: The emission of large amounts of CO_2 into the atmosphere is believed to be a major reason behind climate change, which has led to increased demand for CO_2 capture. Postcombustion CO_2 capture with chemical solvent is considered one of the most important technologies in order to reduce CO_2 emission. Amino acid salt solutions have attracted special attention in recent years due to their excellent physicochemical properties, e.g., low volatility, less toxicity, and high oxidative stability, as well as capture performance comparable with conventional amines. In this study, physicochemical properties of 20 amino acids are reported and their CO_2 absorption performance discussed. The topics covered in this review include the most relevant properties of amino acids including CO_2 loading capacity, cyclic capacity, equilibrium constant, density, viscosity, dissociation constant, CO_2 solubility, CO_2 diffusivity, reaction kinetic between CO_2 and amino acid salts, reaction rate constant, surface tension, heat of CO_2 absorption, precipitation, toxicity, solvent degradation, and corrosion rate. This review provides the most recent information available in the literature on the potential of using amino acid salts as a solvent for CO_2 capture which can help improve the performance of the CO_2 capture process from flue gas streams.

Keywords: amino acid; CO_2 capture; CO_2 emission; gas absorption; global warming.

1 Introduction

The burning of fossil fuels releases a huge amount of greenhouse gases (GHGs) into the atmosphere, which lead to higher temperatures and cause climate change issues (Hu et al. 2016). CO_2 emission as the most important GHG in the atmosphere has to be reduced in order to minimize the consequences of global warming (Jansen et al. 2015). Postcombustion, precombustion, and oxy-fuel combustion are considered promising carbon capture technologies to curtail CO_2 emission (Franca and Azapagic 2015). Among them, CO_2 absorption by a chemical solvent is the most widely employed method (Krupiczka et al. 2015). The selection of a suitable solvent in this method plays a critical role in CO_2 absorption because the performance of process is significantly dependent on the behavior of the solvent (Mondal and Samanta 2019); therefore, several factors such as CO_2 loading capacity, absorption/desorption rate, cyclic capacity, regeneration energy, toxicity, corrosion rate, degradation rate, stability, volatility, and viscosity should be considered (Zarogiannis et al. 2016). Aqueous monoethanolamine (MEA) solution as a primary alkanolamine is the most commonly used absorbent for the CO_2 capture process due to its fast absorption rate and low material price (Liang et al. 2016). However, MEA solution suffers from several limitations such as high degradation rate, low CO_2 loading capacity, toxic nature, and high energy requirement for regeneration, which hinders its industrial utilization (Sreedhar et al. 2017). Therefore, developing new absorbents with better performance than MEA solution is essential to reduce CO_2 capture costs.

Amino acid salt solutions with many advantages such as low toxicity and volatility, good resistance to oxidative and thermal degradation, high surface tension, less corrosive, and fast kinetics with CO_2 are interesting alternatives to MEA solution (Murshid and Butt 2019; Rabensteiner et al. 2014). One of the limitations of amino acid salts is precipitation formation at high CO_2 loading or high concentration. Formation of solid precipitates can cause decrease in mass transfer and damage to equipment. However, the precipitation could have positive

---

***Corresponding author: Rouzbeh Ramezani**, Department of Civil, Chemical and Environmental Engineering, University of Genoa, Via Opera Pia 15, Genova, Italy, E-mail: rouzbeh.ramezani@edu.unige.it
Saeed Mazinani, Department of Chemical Engineering, Centre for Advanced Separations Engineering, University of Bath, Claverton Down, Bath, UK
Renzo Di Felice, Department of Civil, Chemical and Environmental Engineering, University of Genoa, Via Opera Pia 15, Genova, Italy

effects such as lower regeneration energy requirement and higher CO_2 loading if well controlled (Hu et al. 2018). Amino acid salt solutions are generally prepared by neutralizing the amino acid dissolved in deionized water with an equimolar amount of potassium hydroxide (KOH) or sodium hydroxide (NaOH) (Yan et al. 2015). Molecular structures of different types of amino acids are shown in Table 1. Based on a side chain group of amino acids, they can be classified into acidic polar (aspartic acid, glutamic acid), nonpolar (alanine, cysteine, glycine, leucine, methionine, phenylalanine, proline, valine, isoleucine, tryptophan), polar (asparagine, glutamine, serine, threonine, tyrosine), and basic polar (arginine, histidine, lysine).

Favorable properties of amino acid salts make them attractive alternatives to alkanolamine solutions for CO_2 absorption from flue gases. In this regard, many researchers have investigated amino acid salts as a candidate for CO_2 capture and reported their physicochemical properties. Since these studies did not compare performance of amino acid salts to each other, it is difficult to find the best one among 20 different types of amino acids. This motivated us to provide a comprehensive literature review of research works done on CO_2 absorption using amino acid salts to help readers to find the best. To the best of our knowledge, there are only a few review papers in the literature for CO_2 absorption using amino acid salts as listed in Table 2. Hu et al. (2018) and Sefidi and Luis (2019) reviewed latest studies on reaction kinetics between CO_2 and amino acid salt solutions. The vapor-liquid equilibrium (VLE) data and physical properties have not been reported in these reviews. Zhang et al. (2018) provided a brief review of several properties of amino acid salts such as density, viscosity, surface tension, and kinetics. Available review papers are devoted to a few numbers of amino acid salt properties, and there is not a comprehensive review which covers all relevant properties of 20 available amino acids along with their CO_2 absorption performance in detail.

In this review work, the various properties of 20 amino acid salts are discussed in detail in terms of CO^2 loading capacity, cyclic capacity, equilibrium constant, density, viscosity, dissociation constant (pKa), CO^2 physical solubility, CO^2 diffusivity, kinetic study, surface tension, heat of CO^2 absorption, precipitation, toxicity, solvent degradation, and corrosion rate. This review work also focuses on the advantages and disadvantages of each amino acid salt, as well as a comparison of 20 amino acid salts from different aspects. Additionally, absorption performance of amino acid salts is compared to MEA as the most important conventional amine.

2 Amino acid salt properties

2.1 Loading capacity

The CO_2 loading capacity of a solvent which is defined as the number of absorbed CO_2 moles per mole of solvent is one of the most important parameters of an absorbent in the CO_2 capture process. CO_2 loading data at different temperatures, pressures, and solvent concentrations are critical to develop an optimal capture process and helpful in selection of an appropriate solvent (Garg et al. 2017a). For this reason, many publications reported CO_2 loading capacity of amino acid salt solutions at different experimental conditions as listed in Table 3.

For example, Aftab et al. (2018) measured CO_2 loading capacity of 10–30 wt% sodium alaninate (N-Ala) at temperatures of 303–333 K and high CO_2 partial pressures. It was reported that enhancing N-Ala concentration from 10 to 30 wt% and temperature led to a decrease in CO_2 loading capacity. In addition, the authors compared CO_2 loading capacity of 30 wt% N-Ala solution with MEA, 2-amino-2-methyl-1,3-propanediol (AMPD), and sodium glycinate (N-Gly) at the same concentration and 313.15 K and observed that N-Ala has higher CO_2 loading capacity than others at CO_2 partial pressures higher than 15 kPa. They explained that the better performance of N-Ala is due to unstable carbamate formation between CO_2 and N-Ala solution.

In another study, Garg et al. (2016a, 2017a) added NaOH and KOH to phenylalanine in order to prepare sodium and potassium salts of phenylalanine, respectively. They discovered that potassium salt of phenylalanine has a better absorption performance than sodium salt of phenylalanine in terms of CO_2 loading. Moreover, their results showed that 25 wt% K-Phe exhibits higher CO_2 loading capacity than 30 wt% MEA but lower than 30 wt% methyldiethanolamine (MDEA). The authors also claimed that N-Phe can be considered as an attractive solvent at high partial pressure of CO_2. They explained that unstable carbamate formation as a result of the reaction of sodium salt of phenylalanine with CO_2 is converted to bicarbonate and free amine molecules which leads to high CO_2 loading capacity.

Likewise, Kumar et al. (2003a) and Wei et al. (2014) investigated the CO_2 loading capacity of potassium taurate (K-Tau) at temperatures 298–373 K using a stirred-cell reactor (SCR). According to their results, the partial pressure of CO_2 increases when concentration of K-Tau decreases from 6 M to 2 M due to fewer free K-Tau molecules in lower concentrations.

Table 1: Molecular structures of amino acids.

Amino acid	Molecular structure	Amino acid	Molecular structure
Arginine (Arg)	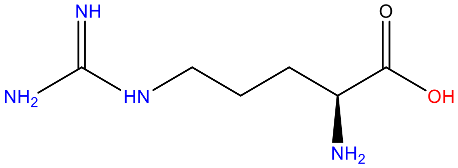	Alanine (Ala)	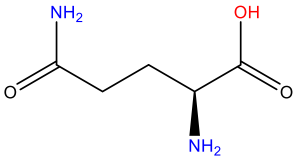
Asparagine (Asp)	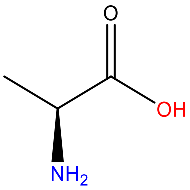	Tyrosine (Tyr)	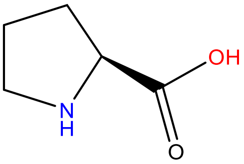
Aspartic acid (Asp acid)	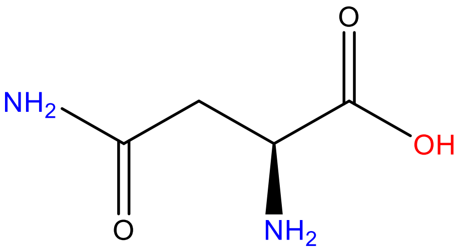	Isoleucine (Iso)	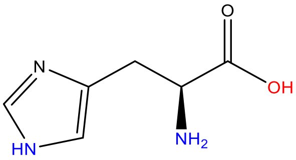
Phenylalanine (Phe)	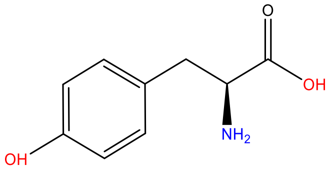	Cysteine (Cys)	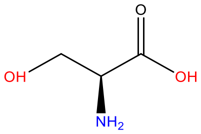
Glutamic acid (Glu acid)	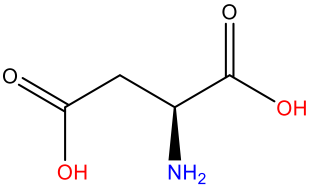	Glycine (Gly)	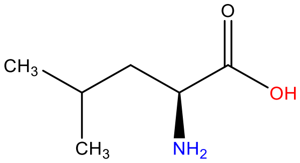
Glutamine (Glu)	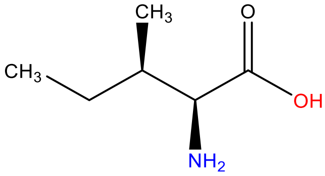	Proline (Pro)	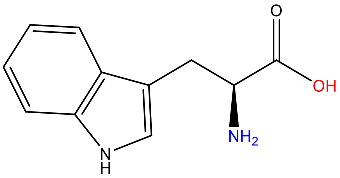
Histidine (His)	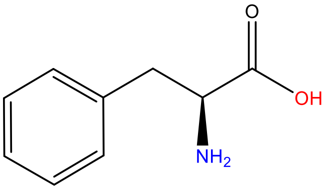	Serine (Ser)	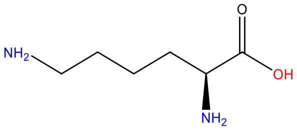

Table 1: (continued)

Amino acid	Molecular structure	Amino acid	Molecular structure
Leucine (Leu)	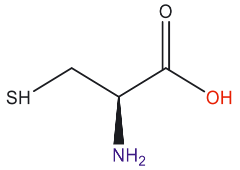	Tryptophan (Try)	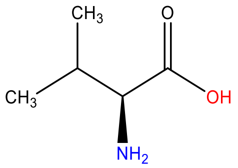
Lysine (Lys)	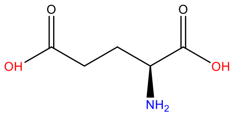	Valine (Val)	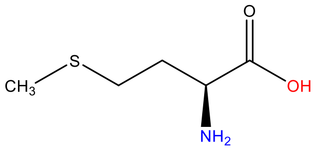
Methionine (Met)	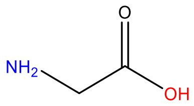	Threonine (Thr)	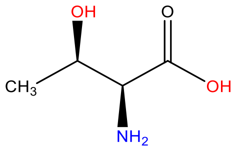

Subsequently, CO_2 loading capacity data in solutions of N-Gly and potassium glycinate (K-Gly) were published by several researchers (Harris et al. 2009; Mondal et al. 2015; Portugal et al. 2009; Song et al. 2006). For example, Song et al. (2006) compared 10 wt% N-Gly solution with MEA, AMPD, and triisopropanolamine (TIPA) at the same concentration and at 313 K. Their results revealed that the CO_2 loading capacity in N-Gly is the highest as compared with the solvents studied. In addition, they indicated that there was no change in the net amount of CO_2 absorbed by N-Gly when the concentration was increased from 20 wt% to 30 wt%. Potassium salts of asparagine (K-Asp) and glutamine (K-Glu) are another two amino acid salts that were evaluated by Chen et al. (2015) at temperatures and CO_2 partial pressures of 313–353 K and 5–950 kPa, respectively. Their experimental results showed that the CO_2 loading capacity of K-Asp and K-Glu decreases when temperature increases from 313 to 353 K due to the exothermic nature of CO_2 absorption. They also compared the absorption performance of CO_2 in K-Glu solution with two conventional alkanolamines at 313.15 K. Their comparison demonstrated that CO_2 loading in 18 wt% K-Glu was higher than 30 wt% MDEA and 30 wt% 2-amino-2-methyl-1-propanol (AMP). Moreover, CO_2 loading capacity was found to be the same for 17 wt% K-Asp and 16 wt % K-Tau solutions, as well as 18 wt% K-Glu and 11 wt% K-Gly solutions.

Majchrowicz and Brilman (2012), Shen et al. (2015), and Chang et al. (2015) obtained CO_2 loading capacity of potassium prolinate (K-Pro). They observed that CO_2 partial pressure has a positive effect on CO_2 loading capacity of the solution due to the increase in the concentration gradient. In addition, a comparison between K-Pro and MEA solutions showed that K-Pro solution has a higher CO_2 loading capacity than MEA only at low partial pressure of CO_2. Proline as a secondary amino acid has an amino group and a distinctive structure of a five-membered ring (Lim et al. 2012).

Aronu et al. (2011a) and Kang et al. (2013) selected 3.5 and 4 M potassium sarcosinate (K-Sar) solutions as an absorbent for CO_2 capture, respectively, and studied its performance at temperatures 313, 333, and 353 K using a vapor-liquid equilibrium apparatus. They have found out that K-Sar presents the lowest CO_2 loading capacity when compared to K-Ala and K-Ser solutions at a CO_2 partial pressure of 15 kPa. This weak performance of K-Sar in comparison to other two amino acid salts is due to its lower basicity ($pK_b = 11.64$) than serine ($pK_b = 9.15$) and alanine ($pK_b = 9.69$). However, all three amino acid salts indicated similar acidity to the carboxyl group at around $pKa = 2.36$.

Table 2: Summary of the reviews done on CO_2 absorption in amino acid salt solutions.

References	Review description
Sefidi and Luis 2019	Review of the reaction kinetics between CO_2 and amino acid salt solutions
Hu et al. 2018	Kinetics study and industrial barriers for implementing amino acid solvent processes
Zhang et al. 2018	A brief overview of physical properties of amino acids

Solutions of potassium serinate (K-Ser) and potassium threonate (K-Thr) were proposed by Song et al. (2011) and Portugal et al. (2009), respectively. According to their observations, 14.3 wt% K-Ser solution has better CO_2 loading capacity than 15 wt% MEA at CO_2 partial pressures above 10 kPa and 313.15 K, while at high temperatures and low CO_2 partial pressure, MEA shows a much better performance.

CO_2 loading experiments in potassium lysinate (K-Lys) solutions were carried out by several researchers (Shen et al. 2015, 2017a; Zhao et al. 2017a). Their results showed that there is no difference between CO_2 loading capacity of 33 and 41 wt% K-Lys. Therefore, the selection of a suitable concentration in this case is necessary to save material cost. Additionally, K-Lys presented a higher CO_2 loading capacity than K-Pro and MEA solutions which can be explained due to their difference in pH of solution and molecular structure. K-Lys has two amino groups which are involved in the reaction with CO_2 while K-Pro and MEA have only one amino group. In addition, K-Lys solution also has higher pH than K-Pro solution, thus K-Lys is more basic than K-Pro. Since carbamate stability decreases with basicity of α-amino group, greater CO_2 loading capacity is expected (Shen et al. 2015).

The CO_2 loading capacity of potassium salts of lysine, proline, alanine, glycine, and taurine was measured Lerche et al. (2012) at temperatures 298, 313, and 323 K, and the results were compared to MEA solution. It was concluded that K-Lys and K-Tau showed the highest and the lowest CO_2 loading capacity, respectively, among the amino acid salts studied. In addition, a higher CO_2 loading capacity for K-Lys in comparison with MEA was also reported which is in good agreement with the finding by Shen et al. (2015).

Table 3: Experimental results for CO_2 loading capacity of different amino acid salt solutions.

Solution	T (K)	Concentration	P_{CO2} (kPa)	CO_2 loading (mol CO_2/mol solution)	References
N-Gly	303–323	10–30 wt%	0.1–200	0.17–1.07	Song et al. 2006
N-Gly	298, 313	1–30 wt%	0–2500	0.5–1.6	Harris et al. 2009
N-Gly	313–333	5–25 wt%	2–600	0.09–1.7	Mondal et al. 2015
K-Gly	293–351	0.1–3 M	0.1–100	0.1–1.4	Portugal et al. 2009
K-Thr	313	1 M	1–42	0.1–0.8	Portugal et al. 2009
K-Asp	313–353	8.5–34 wt%	5–950	0.17–1.22	Chen et al. 2015
K-Glu	313–353	9.2–36.8 wt%	5–950	0.28–1.44	Chen et al. 2015
K-Pro	285, 323	0.5–3 M	0–70	0.5–0.9	Majchrowicz and Brilman 2012
K-Pro	313, 323	2.5 M	0.03–15	0.3–0.7	Shen et al. 2015
K-Pro	313–353	7.5–27.4 wt%	1–1000	0.24–1.16	Chang et al. 2015
K-Lys	313, 333	2.27 M	0.1–18	0.88–1.12	Shen et al. 2015
K-Lys	298–353	9–41.2 wt%	0–110	0.65–1.7	Shen et al. 2017a
K-Lys	313–343	1.25–3.28 mol/kg	0.1–20	0.6–1.2	Zhao et al. 2017a
K-ABA	313–353	6.9–25.6 wt%	1–1000	0.32–1.12	Chang et al. 2015
N-Phe	303–333	10–25 wt%	200–2500	0.2–1.8	Ahn et al. [2010]
K-Phe	303–333	10– 25 wt%	200–2500	0.2–1.9	Garg et al. 2016a
K-Tau	333–373	2–6 M	1–100	0.1–1.1	Wei et al. 2014
K-Tau	298, 313	0.5–4 M	0.2–8	0.2–0.6	Kumar et al. 2003a
N-Ala	303–333	10–30 wt%	200–2500	0.3–1.8	Aftab et al. 2018
K-Ser	313–373	14.3 wt%	0.1–433	0.03–0.99	Song et al. 2011
K-Sar	313–353	4 M	0–938	0.1–0.95	Kang et al. 2013
K-Sar	313–393	3.5 M	0.03–970	0.2–0.8	Aronu et al. 2011a

Chang et al. (2015) observed that potassium aminobutyrate (K-ABA) solution shows different behaviors at different partial pressures of CO_2. When partial pressure of CO_2 is high, CO_2 loading of 13 wt% K-ABA solution is greater than 15 wt% MEA and 14 wt% K-Pro at 313.15 K. However, K-ABA solution absorbs less CO_2 than K-Pro in low partial pressure. The authors explained that this better performance of K-ABA solution is due to bicarbonate formation during reaction with CO_2 while K-Pro produces stable carbamate.

Based on the review above, it was found that amino acid salts solutions have different behaviors at different experimental conditions. In order to have a better analysis of performance of amino acid salts in terms of CO_2 loading capacity, a comprehensive comparison between CO_2 loading capacity of 1 M potassium and sodium salts of various types of amino acids and MEA (Aftab et al. 2018; Chang et al. 2015; Chen et al. 2015; Garg et al. 2016a, 2017a; Kumar et al. 2003a; Lee et al. 1976; Majchrowicz and Brilman 2012; Portugal et al. 2009; Shen et al. 2015, 2017a; Song et al. 2006; Song et al. 2011; Syalsabila et al. 2019) solution was carried out at 313.15 K and a wide range of CO_2 partial pressures as presented in Figure 1. It can clearly be seen that K-Lys has the highest CO_2 loading capacity among all amino acid salt solutions. This can be explained by the fact that this amino acid contains two amino groups in its structure which can absorb more CO_2 (Shen et al. 2015). Potassium salts of glycine, histidine, and glutamine exhibit high CO_2 loading capacity due to more amine functional groups in their structures. Although the CO_2 loading capacity of K-Thr and K-Ser solutions is lower than that of K-Lys, K-Gly, K-His, and K-Glu, their performance is better than others. K-Asp has higher CO_2 loading capacity than K-ABA and K-Pro at high CO_2 partial pressures (Figure 1). In a CO_2 partial pressure range between 10 and 100 kPa, potassium salts of proline and aminobutyric acid have approximately the same CO_2 loading capacity. Potassium taurate indicated the lowest CO_2 loading capacity among the amino acid salts studied. In addition, it is seen from Figure 1 that K-Lys, K-Gly, K-His, and K-Glu have higher CO_2 loading capacity than MEA solution which makes them attractive amino acid salts for CO_2 capture in terms of CO_2 absorption capacity. Additionally, the CO_2 loading capacity of K-Asp, K-Ser, and K-Thr is approximately similar to MEA solution.

The summary of this section is as follows:

- The CO_2 partial pressure has a positive effect on CO_2 loading capacity while temperature has negative effect.
- The formation of unstable carbamate or bicarbonate leads to high CO_2 loading capacity.
- K-Lys and K-Tau exhibit the highest and lowest CO_2 loading capacity among the amino acid salts, respectively.
- K-Lys, K-Gly, K-His, and K-Glu have higher CO_2 loading capacity than MEA solution.
- More amino groups in the structure of amino acids lead to more CO_2 absorption.
- The potassium salt of amino acids has better absorption performance than their sodium salt.
- Greater CO_2 loading capacity can be expected when carbamate stability decreases.

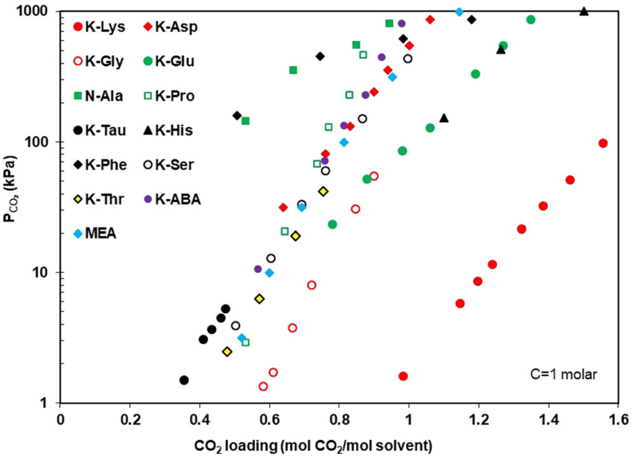

Figure 1: The CO_2 loading capacity of amino acid salt solutions and monoethanolamine (MEA) at 313 K and concentration of 1 kmol/m^3.

2.2 Cyclic capacity

Another important parameter that needs to be considered is cyclic capacity. A solvent with high cyclic capacity is favorable to CO_2 capture because it reduces the size of the column due to reduced absorbent circulation flow rate, thereby reducing process costs (Nwaoha et al. 2017). Values of CO_2 cyclic capacity can be calculated from the difference between the CO_2 loading capacity of solvent after absorption (α_{abs}) and the CO_2 loading of solvent after desorption (α_{des}) according to Eq. (1):

$$\alpha_{cyc} = \alpha_{abs} - \alpha_{des} \tag{1}$$

Song et al. (2012) reported values of cyclic capacity of some amino acid salts at absorption and desorption temperatures of 313.15 and 353.15 K, respectively. They concluded that smaller distances between amino and carboxyl groups and bulkier substituted groups lead to an enhancement of cyclic capacity. In addition, the authors studied the effect of the addition of 0.1 M piperazine to 1 M K-Ala, K-Ser, and K-ABA solutions and observed that an enhancement in net cyclic capacity (mol CO_2/mol solvent) from 0.535 to 0.606 for K-Ala, 0.54–0.609 for K-ABA, and 0.558–0.631 for K-Ser solutions. These blend solutions also showed a higher net cyclic capacity than 1 M MEA solution (0.483 mol CO_2/mol solvent). The strong bonds between CO_2 and MEA which cause a difficult desorption process is the reason for lower cyclic capacity of MEA in comparison with amino acid salt solutions.

Aronu et al. (2010) investigated cyclic capacity of 2.5 M K-Sar solution and compared the results with 2.5 M MEA solution. It was reported that K-Sar has a lower cyclic capacity in comparison with MEA due to the lower equilibrium temperature sensitivity of K-Sar.

CO_2 cyclic capacity of K-Lys at absorption temperature of 313.15 K and desorption temperature of 379.15 K was studied by Zhao et al. (2017b). They used two methods including equilibrium-based and continuous absorption-desorption cycles to calculate the cyclic capacity. According to their results, cyclic capacity value for 33 wt% K-Lys solution, using the continuous-cycle method (0.5 mol CO_2/mol solvent), is lower than values obtained using the equilibrium-based method (0.7 mol CO_2/mol solvent) due to unlimited time to reach equilibrium. Moreover, the authors compared absorption performance of 33 wt% K-Lys (~2 M) with 30 wt% MEA (~5 M) solution. The findings of the study showed a high cyclic capacity for K-Lys, compared to cyclic capacity of MEA solution which is 0.3 (mol CO_2/mol solvent). Based on their results, although the molar concentration of K-Lys is lower than that of MEA, the comparable absorption rate and capacity reveal that the K-Lys has the potential to be considered as an attractive candidate for CO_2 absorption.

Bian et al. (2017) evaluated the cyclic capacity of 27.5 wt% potassium salt of proline at absorption and desorption temperatures of 298.15 and 383.15 K, respectively, and concluded that K-Pro has a higher cyclic capacity ($\alpha_{cyc} = 0.37$) than 30 wt% MEA solution ($\alpha_{cyc} = 0.3$).

A comparison between cyclic capacity of different amino acid salts and MEA solution is shown in Figure 2. It can be observed from this figure that, at concentration of 1 M, the highest and the lowest cyclic capacities among amino acid salts were attained for K-Arg and K-Pro solutions with values of 0.567 and 0.412 (mol CO_2/mol solvent), respectively. The presence of two primary and two secondary amino groups in the structure of K-Arg makes arginine an interesting amino acid in terms of cyclic capacity and CO_2 loading capacity. Although the cyclic capacity of K-Ser was lower than that of K-Arg, this amino acid salt indicated better cyclic capacity (0.558 mol CO_2/mol solvent) than the others. In addition, K-Glu and K-Ala have the same cyclic capacity equal to 0.535 (mol CO_2/mol solvent). K-Tau showed a higher cyclic capacity than K-Gly due to the presence of bulky sulfonic groups in its structure compared to the carboxylic group of glycine (Song et al. 2012).

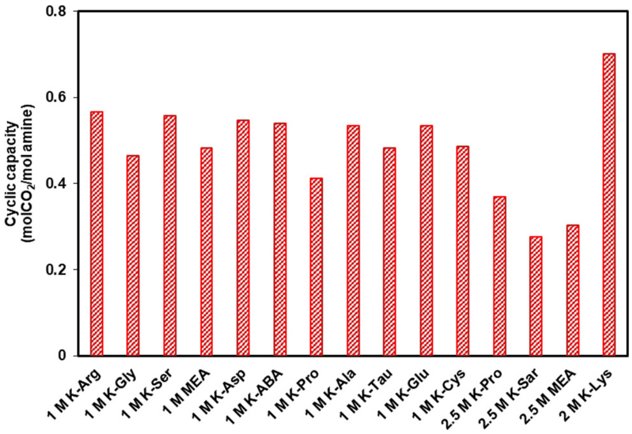

Figure 2: Values of cyclic capacity of CO_2 in different amino acid salts. Data from (Aronu et al. 2010; Bian et al. 2017; Song et al. 2012; Zhao et al. 2017b).

According to Figure 2, potassium salts of arginine, serine, asparagine, aminobutyric acid, alanine, glutamine, cysteine, and taurine might be better choices than MEA because these amino acid salts present larger values of cyclic capacity. At concentrations between 2 and 2.5 M, K-Lys has much higher cyclic capacity (0.7 mol CO_2/mol solvent) than K-Pro (0.37 mol CO_2/mol solvent), K-Sar (0.276 mol CO_2/mol solvent), and MEA (0.303 mol CO_2/mol solvent) solutions. This great performance of K-Lys makes it a favorable candidate for CO_2 absorption from the cyclic capacity point of view. In addition, at this range of concentration, K-Sar indicated the lowest cyclic capacity value due to its poor desorption performance which leads to a higher regeneration cost.

The key messages of this section can be summarized as follows:

- The smaller distances between amino and carboxyl groups and bulkier substituted groups result in an enhancement in cyclic capacity.
- Amino acid salts with bulky sulfonic groups have better cyclic capacity.
- Strong bonds between CO_2 and the amino group have negative effect on cyclic capacity.
- K-Arg, K-Ser, K-Asp, and K-Lys are favorable candidates for CO_2 absorption from the cyclic capacity point of view.

2.3 Equilibrium constants

The modeling studies and prediction of CO_2 loading capacity data in amino acid salt solutions are important to determine the partial pressure of CO_2 and efficient design of an absorption column (Aronu et al. 2011a). In order to develop the thermodynamic models and predict equilibrium data, values of equilibrium constants for reactions between CO_2 and amino acid salt solutions are required (Suleman et al. 2018). The constants of amino acid deprotonation (K_1) and carbamate hydrolysis (K_2) of different amino acid salt solutions are listed in Table 4. The reaction between amino acid salt solutions and CO_2 can be described as follows (Yang et al. 2014a; Zhang et al. 2018):

$$H_3N^+RCOO^- \leftrightarrow^{K_1} H_2NRCOO^- + H^+ \tag{2}$$

$$COORNHCOO^- + H_2O \leftrightarrow^{K_2} H_2NRCOO^- + HCO_3{}^- \tag{3}$$

$$H_2O + CO_2 \leftrightarrow^{K_3} H^+ + HCO_3{}^- \tag{4}$$

$$H_2O \leftrightarrow^{K_4} H^+ + OH^- \tag{5}$$

$$HCO_3{}^- \leftrightarrow^{K_5} H^+ + CO_3^{2-} \tag{6}$$

Several models are available in the literature to analyze vapor-liquid equilibrium in the water + amine + CO_2 systems and to predict the equilibrium solubility of CO_2 in the solution (Shen et al. 2017a). Among them, a Kent-Eisenberg model (Kent and Eisenberg 1976), as a function of temperature, is a widely used thermodynamic model due to its computational simplicity and the fact that the Kent-Eisenberg model was one of the firstly developed models. Li and Shen (1993) and Hu and Chakma (1990) proposed the modified Kent-Eisenberg models as a function of pressure, temperature, and concentration.

Nowadays, more complex methods are usually applied to describe the thermodynamics of the CO_2 absorption in chemical solvents. For example, the extended UNIQUAC model and Deshmukh-Mather model are based on activity coefficient approach. The electrolyte-NRTL activity coefficient model proposed by Chen et al (Chen et al. 1979, 1982; Chen and Evans 1986) is one of the most accurate thermodynamic models which is based on excess Gibbs energy. The universal quasichemical (UNIQUAC) and non-random two-liquid (NRTL) models are able to represent the phase equilibrium of highly nonideal nonelectrolyte solutions (Mock et al. 1986). Many researchers used these models to predict CO_2 loading capacity of amino acid salt solutions.

Chen et al. (2015), Chang et al. (2015), and Shen et al. (2017a) applied a modified Kent-Eisenberg model for CO_2 absorption in solutions of K-Asp, K-Pro, and K-Lys, respectively. First, initial guess values were set for equilibrium constants and then concentrations of the liquid phase species in amino acid salt solutions were calculated at different temperatures, CO_2 loading capacity, and solvent concentrations based on charge and mass balances. By minimizing the objective function ($F_{obj} = (P_{CO2}^{exp} - P_{CO2}^{cal}/P_{CO2}^{exp})^2$) between modeling results and experimental data, the values of equilibrium constant can be determined at different operating conditions. Next, the calculated equilibrium constants were regressed as a function of CO_2 loading, temperature, and concentration by the least square method.

Shen et al. (2017a) predicted the concentration of the liquid phase species in K-Lys solution at 313.2 K using the proposed model to provide a better understanding of the absorption process. It was concluded that at CO_2 loading of up to 0.7, values of carbamate, carbonate, and LysH increase while value of Lys^- decreases. As the CO_2 loading increases, LysH gradually decreases and the corresponding protonated lysine increases. Bicarbonate can be considered as one of main species formed at high CO_2 loading due to the hydrolysis of carbamates.

Garg et al. (2017a) and Aftab et al. (2018) developed a modified Kent-Eisenberg model as a function of pressure, temperature, and concentration to predict CO_2 loading capacity of N-Ala and N-Phe solutions, respectively. Average absolute deviations (AADs) were found to be equal to 12.8 and 8.7% for N-Ala and N-Phe, respectively. Garg et al. (2017a) also compared performance of a modified Kent-Eisenberg model with an artificial neural network (ANN) technique. The Levenberg-Marquardt algorithm was applied in the artificial neural network model to simulate the experimental CO_2 loading capacity of N-Phe solution. The objective of the training procedure is to minimize the error between the experimental CO_2 loading and model results. The mean square error ($\frac{1}{N}\sum_{N-1}^{N}(X_{Pred} - X_{exp})^2$) is criteria applied for minimizing the error. They observed that the ANN model has a better performance for predicting CO_2 loading capacity than a modified Kent-Eisenberg model. The AAD of the predicted CO_2 loading capacity using a Kent-Eisenberg model was 8.7%, while the AAD using the ANN technique was 3% which proves the accuracy of the ANN model.

The modified Kent-Eisenberg model proposed by Mondal et al. (2015) was used to correlate the equilibrium constants in CO_2 + N-Gly + H_2O system included concentration and temperature parameters. The authors reduced the charge balance, mass balance, and equilibrium constant equations to a single five-order polynomial equation as a function of hydrogen ion concentration. The root of this equation which is in the range of 10^{-6}–10^{-12} is considered as hydrogen ion concentration. Then, concentration of all liquid phase species in the solution, as well as CO_2 loading, can be calculated. The equilibrium constants were regressed as a function of temperature and concentration

Table 4: The reaction equilibrium constants of CO_2 and amino acid salts.

Solution	Equilibrium constant	References
	K_1 (amine deprotonation)	
N-Gly	$K = 3.77 \times 10^{-8} - 4.69 \times 10^{-9} \times C - 2.109 \times 10^{-10} \times T + 1.603 \times 10^{-11} \times C \times T + 2.844 \times 10^{-13} \times T^2$	Mondal et al. 2015
K-Asp	$K = \exp(26.341 - 1.15 \times 10^4/T - 1.901 \times 10^6/T^2 + 1.215 \times \alpha - 3.159 \times \alpha^2 + 3.106 \times C)$	Chen et al. 2015
K-Glu	$K = \exp(-289.69 + 18.71 \times 10^4/T - 33.334 \times 10^6/T^2 + 8.823 \times \alpha - 3.14 \times \alpha^2 + 1.844 \times C)$	Chen et al. 2015
K-Pro	$K = \exp(11.601 + 6049/T - 722890/T^2 - 25.001 \times \alpha + 3.512 \times \alpha^2 - 3.713 \times C)$	Chang et al. 2015
K-Lys	$K = \exp(-453.07 + 18319/T + 71.018 \times \ln(T) - 5.751 \times \alpha - 61.612/\alpha + 35.39/\alpha^2 - 0.622 \times C)$	Shen et al. 2017a
K-Lys	$K' = \exp(-76.36 + 1013.2/T + 3.828 \times \ln(T) + 8.039 \times \alpha + 25.8265/\alpha - 7.67/\alpha^2 - 0.038 \times C)$	Shen et al. 2017a
N-Ala	$K = 3.8 \times 10^{-8} + 4.1 \times 10^{-9} \times C - 4.8 \times 10^{-11} \times T + 6.09 \times 10^{-11} \times T \times C - 4.3 \times 10^{-13} \times T^2 - 8.6 \times 10^{-15} \times P + 4.9 \times 10^{-18} \times P^2$	Aftab et al. 2018
N-Phe	$K = 4.7 \times 10^{-8} - 4.18 \times 10^{-10} \times C - 5.63 \times 10^{-11} \times T + 1.07 \times 10^{-11} \times C \times T + 1.44 \times 10^{-13} \times T^2 + 8.17 \times 10^{-16} \times P + 9.99 \times 10^{-19} \times P\text{\textasciicircum}2$	Garg et al. 2017a
K-Sar	$K = \exp(-5.9752 - 5185.1/T)$	Aronu et al. 2011a
	K_2 (carbamate hydrolysis)	
N-Gly	$K = 5.775 - 0.050 \times C - 0.034 \times T - 0.018 \times C^2 + 0.0004 \times C \times T + 5 \times 10^{-5} \times T^2$	Mondal et al. 2015
K-Asp	$K = \exp(9.025 + 1.25 \times 10^4/T - 5.047 \times 10^6/T^2 - 3.481 \times \alpha - 4.132 \times \alpha^2 + 1.145 \times C)$	Chen et al. 2015
K-Glu	$K = \exp(-315.28 + 21.95 \times 10^4/T - 38.329 \times 10^6/T^2 + 3.816 \times \alpha - 3.003 \times \alpha^2 + 1.371 \times C)$	Chen et al. 2015
K-Pro	$K = \exp(-22.245 - 3869/T - 370270/T^2 - 29.222 \times \alpha - 14.393 \times \alpha^2 + 4.745 \times C)$	Chang et al. 2015
K-Lys	$K = \exp(-66.53 + 1850.4/T + 6.398 \times \ln(T) + 6.764 \times \alpha + 22.001/\alpha - 6.593/\alpha^2 - 0.042 \times C)$	Shen et al. 2017a
K-Lys	$K = \exp(178.01 - 12014/T - 38.759 \times \ln(T) + 19.901 \times \alpha + 112.45/\alpha - 50.268/\alpha^2 - 0.010 \times C)$	Shen et al. 2017a
N-Ala	$K = -9.5 - 0.05 \times C - 0.005 \times T - 0.06 \times C^2 + 3.1 \times 10^6 \times T \times C + 1.3 \times 10^{-5} \times T^2 + 5.4 \times 10^{-7} \times P + 2.1 \times 10^{-8} \times P^2$	Aftab et al. 2018
N-Phe	$K = 1.1 - 0.007 \times C - 0.001 \times T - 0.0008 \times C^2 + 0.0001 \times C \times T + 9 \times 10^{-6} \times T^2 + 1.1 \times 10^{-6} \times P + 1 \times 10^{-8} \times P^2$	Garg et al. 2017a
K-Sar	$K = \exp(-7.4569 + 0.9753/T)$	Aronu et al. 2011a

to fit the experimental CO_2 loading with the Kent-Eisenberg model prediction. In order to minimize the error between the experimental and modeling results, a generalized reduced gradient nonlinear optimization technique was used. This technique was successfully employed by many researchers in the literature as a suitable method. Their results showed that this model is able to correlate experimental data with an AAD of around 7%.

Aronu et al. (2011a) used the UNIQUAC model to predict CO_2 loading capacity of K-Sar solution. The model is assumed to be dependent on temperature. The UNIQUAC model has three terms, including an electrostatic term of the Debye-Huckel type, a residual, and a combinatorial term. The authors used these terms to regress equilibrium constant. The Levenberg-Marquardt minimization using MATLAB software based on parameter estimation tool (Modfit) was used in their work for regression analysis. The finding of their study demonstrates that this UNIQUAC model gives good agreement between model results and experimental data with an AAD of 5.5%.

Based on the results above, the modified Kent-Eisenberg model, UNIQUAC model, and ANN model are able to predict reasonably the equilibrium solubility of CO_2 in amino acid salt solutions. In comparison with the UNIQUAC model and ANN model, the modified Kent-Eisenberg model is a simple model and has high speed of computation. Although the modified Kent-Eisenberg model has reasonable prediction capability, its AAD is higher than that of UNIQUAC and ANN because in the modified Kent-Eisenberg model, the activity coefficients of chemical species in amino acid solutions were neglected. AAD of different thermodynamic models was listed in Table 5. Moreover, the modified Kent-Eisenberg model shows a poor agreement at low CO_2 loading and at outside the validity range. The UNIQUAC model and ANN model give better fit than the modified Kent-Eisenberg model. However, they need a greater number of adjustable parameters and many nonlinear system of equations which lead to complexity of these models.

2.4 Density and viscosity

The values of density and viscosity of amino acid salt solutions are necessary for the design of gas-liquid contactors in the absorption process (Garg et al. 2017b; Shaikh et al. 2015a). In the last few years, many researchers have measured the density and viscosity of amino acid salt solutions at different temperatures and concentrations. The experimental data of density and viscosity of some amino acid salts are presented in Table 6.

Garg et al. (2016a) showed that density reduces with a rise in temperature. The space between amino acid molecules increases at higher temperatures while the mass stays constant, thus decreasing the density. It was also found that the density increases when increasing the concentration of amino acid salts because of the higher availability of amino acids molecules (Shaikh et al. 2017). Shaikh et al.

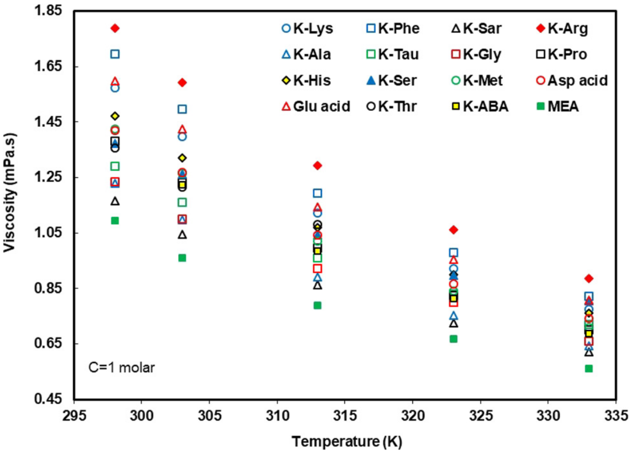

Figure 3: Viscosity of 1 M amino acid salt solutions as a function of temperature.

Table 5: Summary of different models used in the literature to predict CO_2 loading.

References	Model	Parameters	AAD %
Mondal et al. 2015	Modified Kent-Eisenberg model	T, C	7.13
Chen et al. 2015	Modified Kent-Eisenberg model	T, C, CO_2 loading	10.3 – 12.8
Chang et al. 2015	Modified Kent-Eisenberg model	T, C, CO_2 loading	13.1 – 15
Shen et al. 2017a	Modified Kent-Eisenberg model	T, C, CO_2 loading	3.2
Aftab et al. 2018	Modified Kent-Eisenberg model	T, C, P_{CO2}	12.8
Garg et al. 2017a	Modified Kent-Eisenberg model	T, C, P_{CO2}	8.75
Garg et al. 2017a	Artificial neural network model	T, C, P_{CO2}	2.99
Aronu et al. 2011a	UNIQUAC model	T	5.5

AAD: average absolute deviation.

Table 6: Experimental results for density and viscosity of different amino acid salt solutions.

Solution	T (K)	Concentration	Density (g/cm^3)	Viscosity (mPa.s)	References
K-Lys	298 – 313	0.5–2.5 M	1.0307–1.1738	0.894–3.1652	Mazinani et al. 2015
K-Lys	298, 313	2, 2.5 M	1.1091–1.1419	2.351–5.544	Zhao et al. 2017b
K-Lys	293–353	0.2–3.6 mol/kg	0.989–1.145	0.426–6.645	Bian et al. 2016
K-Lys	298–333	0.26–1.98 M	1.0008–1.1168	0.550–3.557	Shen et al. 2016c
K-Lys	298–348	0.2–3 M	0.987–1.151	0.435–8.407	Shen et al. 2015
K-Pro	298–348	0.5–3 M	1.0056–1.1669	0.473–4.053	Shen et al. 2015
N-Pro	298–343	5–40 wt%	0.995–1.148	0.461–5.56	Shaikh et al. 2014
K-Pro	303–323	0.5–3.03 M	1.012–1.167	0.667–3.46	Paul and Thomsen 2012
K-Pro	298–333	0.5–3.4 M	1.014–1.197	0.565–5.732	Holst et al. 2008
K-Arg	298–323	0.26–1.23 M	1.0048–1.1066	0.549–2.085	Shen and Yang 2016a
K-Arg	293–353	0.26–1.15 mol/kg	0.995–1.086	0.405–1.923	Bian et al. 2016
K-Arg	298–333	0.23–0.97 M	1.007–1.087	0.539–1.882	Holst et al. 2008
K-Sar	298–353	1–7 M	1.0201–1.3118	0.593–4.578	Aronu et al. 2012
K-Sar	298–333	0.5–2.9 M	1.01–1.15	0.538–2.493	Holst et al. 2008
K-His	298–340	0.26–1.97 M	1–1.15	0.5–3	Shen et al. 2016b
K-His	293–353	0.26–2.55 mol/kg	0.993–1.153	0.401–3.047	Bian et al. 2016
N-Gly	313–333	5–25 wt%	1.01–1.12	0.58–1.59	Mondal and Samanta 2019
N-Gly	303–353	10–50 wt%	1.0082–1.2066	0.63–4.413	Lee et al. 2005
K-Gly	293–313	0.1–2.98 M	0.9972–1.168	0.666–2.109	Portugal et al. 2008
N-Gly	298–343	1–17 wt%	0.983–1.097	0.449–2.052	Shaikh et al. 2015b
N-Gly	298–353	1–30 wt%	0.9853–1.1304		Harris et al. 2009
K-Ser	298	1.5 M	1.0687		Kang et al. 2013
K-Ser	298–353	7–57 wt%	1.007–1.263	0.494–4.202	Song et al. 2011
K-Ala	298–333	0.5–3.5 M	1.011–1.181	0.546–3.245	Holst et al. 2008
K-Ala	293–313	1–3 M	1.048–1.16	1.041–3.291	Kim et al. 2012
K-Tau	293–353	2–6 M	1.11–1.39	0.766–10.5	Wei et al. 2014
Glu acid	298–333	0.24–1.46 M	1.017–1.173	0.535–2.194	Holst et al. 2008
K-Met	298–333	0.25–1.47 M	1.003–1.1	0.51–1.88	Holst et al. 2008
K-Phe	298–333	0.25–1.45 M	1.001–1.1	0.549–2.483	Holst et al. 2008
K-Phe	298–343	5–25 wt%	0.991–1.077	0.419–1.717	Garg et al. 2016b
Asp acid	298–333	0.25–1.45 M	1.015–1.176	0.525–1.856	Holst et al. 2008
K-ABA	303–343	0.1–6 wt%	1.001–1.131	0.514–4.954	Garcia et al. 2015
K-Thr	293–313	0.1–3 M	1–1.192	0.683–5.116	Portugal et al. 2008
K-Thr	293–313	0.3–1 M		0.782–1.509	Hwang et al. 2010

(2014) investigated the effect of temperature on viscosity of amino acid salt solutions and concluded that temperature has a significant effect on viscosity at high amino acid salt concentrations. In addition, the viscosity of amino acid salts increases as concentration increases. The reason is that as the concentration increases, collisions between the molecules increase due to the availability of a higher number of molecules (Shaikh et al. 2015b).

The viscosity of potassium salt of 15 different types of amino acids as a function of temperature was plotted in Figure 3. The data have been taken from (Aronu et al. 2012; Garcia et al. 2015; Hartono et al. 2014; He et al. 2017; Holst et al. 2008; Portugal et al. 2017, 2008; Shen et al. 2015, 2016b; Shen and Yang 2016a; Song et al. 2011). As seen from this figure, the viscosity of amino acid salts is a strong function of temperature. For example, when temperature increases from 298 to 333 K, the viscosity of K-Phe and K-Lys solutions decreases by 52 and 51%, respectively, which makes their application more practical at high temperature. In other words, since viscosity affects mass transfer, amino acid salt solutions with low viscosity benefit from the diffusion coefficient of CO_2 in the liquid phase, which results in low mass transfer resistance.

Figure 3 also indicates that the potassium salt of arginine presents the highest viscosity as compared with others, and potassium salt of phenylalanine shows the second highest viscosity. It is evident that K-Sar exhibited the lowest viscosity, which is good from the industrial point of view. In addition, potassium salts of methionine and aspartic acid and potassium salts of proline and aminobutyric acid offer similar viscosity values.

A comparison of viscosity of amino acid salt solutions and MEA at different temperatures was also made. In comparison with MEA, amino acid salts showed slightly higher viscosity. Therefore, the viscosity of potassium salt of amino acids can be ranked in the following order: arginine > phenylalanine > glutamic acid > lysine > histidine > methionine ≈ aspartic acid serine > proline ≈ aminobutyric acid > taurine > glycine > alanine > sarcosine > MEA.

The density of different amino acid salt solutions was depicted in Figure 4. The density of amino acid salt solutions linearly decreases as temperature increases. It is observed that the effect of temperature on density of amino acid salts is insignificant. For instance, the density of potassium salt of histidine decreases from 1.084 to 1.07 (g/cm^3) as temperature increases from 298 to 333 K.

Potassium salts of aspartic acid and glutamic acid presented the highest density, while potassium salts of sarcosine and aminobutyric acid indicated the lowest. In summary, the density of potassium salt of amino acids follows the order: aspartic acid > glutamic acid > arginine > histidine > serine > methionine >
phenylalanine ≈ threonine > lysine > proline ≈ glycine >
alanine > aminobutyric acid > sarcosine.

The summary of this section is as follows:

- The viscosity of amino acid salts is a strong function of temperature and concentration.
- K-Arg presents the highest viscosity while K-Sat has the lowest.
- In comparison with MEA, amino acid salts showed slightly higher viscosity.
- The effect of temperature on density of amino acid salts is insignificant.

2.5 Dissociation constant

The pKa is another parameter of solvent that should be taken into consideration because of its effect on the reaction kinetics of CO_2 with solvent (Bernhardsen and Knuutila 2017; Perinu et al. 2018). The values of pKa of amino acid salts (Holst et al. 2009; Hu et al. 2017a; Kim et al. 2012; Kumar et al. 2003b; Majchrowicz et al. 2014a; Portugal et al. 2017, 2008; Shen et al. 2016b, 2016c; Shen and Yang 2016a; Simons et al. 2010; Yang et al. 2014a; Zhang et al. 2018) along with MEA (Shen et al. 2016b) and MDEA (Hamborg et al. 2007) solutions at a temperature of 298.15 K are presented in Figure 5. It can clearly be seen that K-Lys has the highest pKa among all amino acid salt solutions. K-Pro and K-Sar are other amino acid salts which exhibit higher pKa than others. Therefore, faster CO_2 absorption kinetics for these three amino acid salts can be expected due to their high pKa values. Moreover, pKa values were found to be the same for aminobutyric acid, leucine, and alanine, as well as aspartic acid and glutamic acid. Although the asparagine indicated the lowest pKa among all the amino acid salts, its pKa was still greater than that of MDEA.

According to Figure 5, arginine shows a lower pKa than alanine, while arginine presents higher reaction rate than alanine. It should be noted that pKa is not the only factor which affects reaction kinetics. The reaction rate constant needs to be also considered as an important factor which affects reactivity of absorbents with CO_2. The pKa value can only give guidance to preliminary estimation of the reaction kinetics (Li et al. 2015).

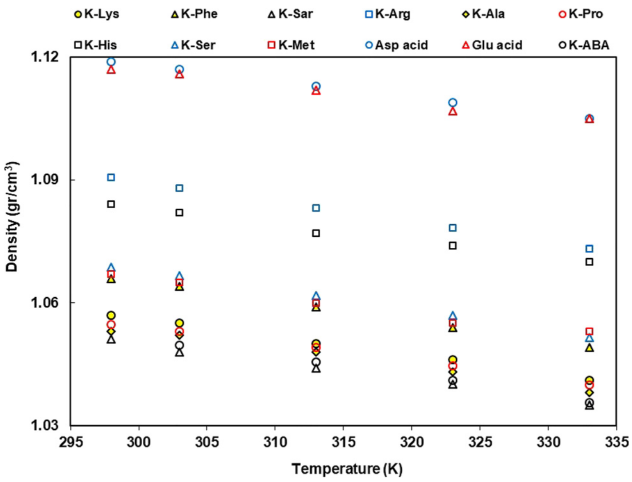

Figure 4: Density of 1 M amino acid salt solutions as a function of temperature.

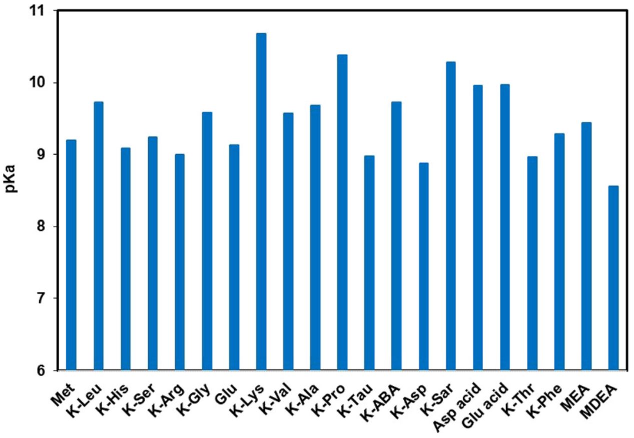

Figure 5: pKa values of amino acid salts at 298 K in diluted solutions. pKa, dissociation constant.

It is evident from comparison made in Figure 5 that most amino acid salts have a greater pKa than MEA, which shows high reactivity of the amino group in their structure with CO_2. Moreover, all amino acid salts offer a higher pKa value than MDEA. In summary, pKa of amino acid salts can be ranked as follows: K-Lys > K-Pro > K-Sar > Glu acid > Asp acid > K-ABA > K-Leu > K-Ala > K-Gly > K-Val > K-Phe > K-Ser > Met > Glu > K-His > K-Arg > K-Tau > K-Thr > K-Asp.

Yang et al. (2014a) reported the pKa values of potassium salt of alanine, valine, aminobutyric acid, taurine, proline, glycine, and sarcosine at a temperature range of 298–353 K. These data were shown in Figure 6 to better analyze the performance of amino acid salts in terms of pKa at high temperatures. It can clearly be seen that as temperature increases from 298 to 353 K, pKa of K-Sar, K-Pro, K-Gly, K-Tau, K-ABA, K-Val, and K-Ala decreases by 8.1, 12.1, 14.6, 15.5, 12.8, 13.9, and 13.6%, respectively. Therefore, sarcosine showed less variation in pKa with temperature compared to others. In addition, sarcosine exhibited the highest pKa at all temperatures except at 298 K, that is, very similar to pKa of proline. It can therefore be concluded that using potassium salt of sarcosine for CO_2 capture at high temperature might be a right choice.

The important conclusions of this section are as follows:

- pKa and reaction rate constant are two important factors which affect reaction kinetics.
- Among amino acid salts, K-Sar showed less variation in pKa with temperature.
- pKa of amino acid salts decreases as temperature increases.
- K-Sar exhibits higher pKa than other amino acid salts at high temperatures.
- K-Lys, K-Pro, and K-Sar showed high pKa value.
- All amino acid salts offer higher pKa value than MDEA solution.

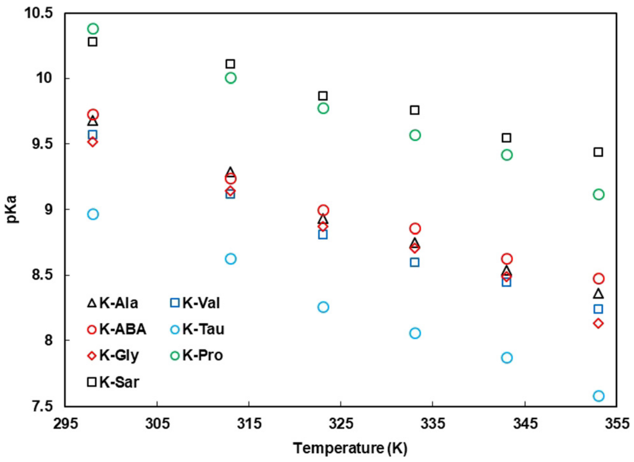

Figure 6: pKa of amino acid salt solutions as a function of temperature. Data from (Yang et al. 2014a). pKa, dissociation constant.

2.6 Henry's constant and diffusivity of CO_2

Henry's law describes the amount of CO_2 that can dissolve in a solvent. This is directly proportional to the partial pressure of the gas in equilibrium with the liquid (Hairul et al. 2016). In addition, the values of Henry's constant (H_{CO2}) and diffusivity of CO_2 (D_{CO2}) in amino acid salt solutions are necessary to calculate the kinetics and the liquid-side mass transfer coefficient. The H_{CO2} and D_{CO2} of several amino acid salts at different temperatures and concentrations are listed in Table 7. According to the results reported in the literature, the diffusivity of CO_2 in amino acid salt solutions increases as the temperature increases and decreases when concentration increases.

2.7 Reaction kinetics between CO_2 and amino acid salts

An ideal solvent for CO_2 capture should have a faster absorption rate because it leads to shorter column sizes, thus reducing the capital cost of the absorber (Shen et al. 2016c). The most widely used techniques to investigate reaction kinetics of CO_2 with chemical absorbents are the string of discs contactor, wetted-wall column (WWC), SCR, and stopped-flow technique (Yu et al. 2017). Many researchers used these techniques to study the kinetics of CO_2 absorption in amino acid salt solutions. A brief summary of their results is listed in Table 8.

Mahmud et al. (2017) measured the rate of CO_2 absorption in three amino acids including sarcosine, glycine, and arginine at temperatures of 293–313 K and concentrations of 0.05–2 M using the stopped-flow technique. Reaction order with respect to Gly, Sar, and Arg was reported to be 1, 1.22, and 1.2, respectively, which means zwitterion formation is rate determining. It was also found that the effect of hydroxyl ion in the formation of carbamate for Gly + CO_2 and Arg + CO_2 systems is negligible while this effect is significant for Sar + CO_2 system. Guo et al. (2013) determined kinetics data of CO_2 absorption in 0.5–2 M K-Gly solution using the stopped-flow technique and WWC. They concluded that the absorption rate using the stopped-flow technique shows slower values in comparison with the WWC.

Table 7: Experimental data of diffusivity and Henry's law constant of CO_2 in amino acid salt solutions.

Solution	T (K)	Concentration	H_{CO2} (kPa.m^3/kmol)	D_{CO2} (m^2/s)	References
N-Gly	303–323	1.05–3.46 M	3539–5709	1.35–2.33	Lee et al. 2007
K-Gly	293–313	0.1–3 M	2710–7554	0.94–2.66	Portugal et al. 2017
K-Thr	293–313	0.1–3 M	2442–8046	0.4–2.61	Portugal et al. 2008
K-Ala	293–313	1–3 M	3546–8840	0.83–2.14	Kim et al. 2012
K-Lys	298–333	0.26–1.98 M	3317–7245	0.56–3.52	Shen et al. 2016c
K-Pro	303–323	0.5–3 M	3817–9427		Paul and Thomsen 2012
K-Sar	298–333	1–4 M	4540–15,020	0.59–3.14	Aronu et al. 2011b
K-His	298–333	0.27–2.07 M	3182–9899	0.95–3.88	Shen et al. 2016b
K-Arg	298–333	0.27–1.23 M	3379–8190	1.15–3.68	Shen and Yang 2016a

Table 8: A summary of kinetics studies of CO_2 absorption in different amino acid salt solutions.

Solution	Apparatus	T (K)	Concentration	Kinetic equation	Order	E (kJ/mol)	References
N-Gly	WWC	303–323	1–3.5 M	$1.95 \times 10^{13} \exp(-7670/T)$	1	63.8	Lee et al. 2007
K-Gly	SCR	293–303	0.1–3 M	$2.81 \times 10^{10} \exp(-5800/T)$	1	48.2	Portugal et al. 2017
K-Gly	Stopped-flow	298–313	0.5–2 M	$1.24 \times 10^{12} \exp(-5459/T)$	1	45.4	Guo et al. 2013
K-Gly	WWC	323, 333	0.5–2 M	$8.18 \times 10^{12} \exp(-8624/T)$	1	71.7	Guo et al. 2013
K-Gly	WWC	313–353	2 M	$1.22 \times 10^{12} \exp(-5434/T)$	1	45.2	Thee et al. 2014
K-Gly		275–355		$3.77 \times 10^{13} \exp(-6568/T)$	1	54.6	Hu et al. 2018
N-Gly	SCR	298–318	0.5–3 M	$3.82 \times 10^{12} \exp(-7188/T)$	1	59.8	Park et al. 2008
Gly	Stopped-flow	293–313	0.05–2 M	$3.29 \times 10^{13} \exp(-8143/T)$	1	67.71	Mahmud et al. 2017
K-Sar	SCR	298–308	0.5–3.8 M	$8.67 \times 10^{8} \exp(-3127/T)$	1.66	26	Simons et al. 2010
N-Sar	Stopped-flow	288 – 318		$9.45 \times 10^{14} \exp(-7337/T)$		61	Xiang et al. 2012
Sar	Stopped-flow	293–313	0.05–2 M	$3.90 \times 10^{13} \exp(-7991/T)$	1.22	66.44	Mahmud et al. 2017
K-Sar	SDC	298–333	1–4 M	$2.61 \times 10^{9} \exp(-915.8/T)$	1.2–1.8		Aronu et al. 2011b
K-Pro	SCR	290–303	0.5–3 M	$3.69 \times 10^{12} \exp(-43330/RT)$	1.4–1.44	43.3	Majchrowicz et al. 2014a
K-Pro	WWC	303–323	0.5–3 M	$2.42 \times 10^{11} \exp(-36452/R\,T)$	1.3–1.4	36.5	Paul and Thomsen 2012
K-Pro	SCR	298	0.74–1.65		1.08		Holst et al. 2009
N-Pro	Stopped-flow	298 – 313	0.01	$5.28 \times 10^{5} \exp(-1440/T)$	1	12	Sodiq et al. 2014
K-Thr	SCR	298–313	0.1–3 M	$4.13 \times 10^{8} \exp(-3580/T)$	1	40.6	Portugal et al. 2008
K-Thr	SCR	293–313	0.1–1 M	$3.95 \times 10^{9} \exp(-4883/T)$	1	40.6	Hwang et al. 2010
His	Stopped-flow	298 – 313	0.01 M	$4.43 \times 10^{12} \exp(-6292/T)$	1.18	52.3	Hu et al. 2017b
K-His	WWC	298–333	0.26–2.07 M	$9.13 \times 10^{8} \exp(-3121/T)$	1.33	25.9	Shen et al. 2016b
K-Lys	WWC	298–333	0.25–2 M	$2.77 \times 10^{13} \exp(-6138/T)$	1.58	51	Shen et al. 2016c
K-Ala	SCR	293–313	1–3 M	$4.51 \times 10^{8} \exp(-3845/T)$	1		Kim et al. 2012
K-Arg	WWC	298–333	0.26–1.23 M	$6.47 \times 10^{5} \exp(-731/T)$	1.2–1.6		Shen and Yang 2016a
Arg	Stopped-flow	293–313	0.05–2 M	$2.81 \times 10^{10} \exp(-4482/T)$	1.22	37.28	Mahmud et al. 2017
N-Tau	Stopped-flow	298–313		$5.44 \times 10^{11} \exp(-5780/T)$	1	48.1	Sodiq et al. 2014
K-Tau	SCR	285–305		$3.23 \times 10^{12} \exp(-5700/T)$	1–1.5	47.3	Kumar et al. 2003b
K-Tau	WWC	323–353		$2.7 \times 10^{12} \exp(-6074/T)$	1	50.5	Wei et al. 2014

WWC: wetted-wall column; SCR: stirred-cell reactor, SDC: string of discs contactor, Order: reaction order with respect to amino acid.

A string of discs contactor was used by Aronu et al. (2011b) to study reaction kinetics between CO_2 and K-Sar at temperatures of 298–333 K and where the concentration was varied between 1 and 4 M. It was concluded that the reaction order varies from 1.25 to 1.81 when the concentration of K-Sar increases. The kinetics of CO_2 absorption in potassium salt of histidine at temperatures and concentrations ranging from 298 to 333 K and 0.2 to 2 M, respectively, using a WWC were investigated by Shen et al. (2016b). The findings of this study showed that K-His has a faster CO_2 absorption rate than MEA solution but lower than K-Lys, K-Sar, K-Pro, and K-Gly solutions. The reaction order was also found to be between 1.22 and 1.45 with activation energy equal to 25 kJ/mol.

Kim et al. (2012) studied CO_2 absorption rate in 1–3 M K-Ala solution using an SCR. The authors observed absorption rate increases as the temperature and concentration of amino acid salt increases. Wei et al. (2014) proposed potassium salt of taurine and evaluated its absorption rate performance at temperatures up to 353 K using a WWC. They reported values of reaction order with respect to K-Tau and activation energy equal to 1 and 50.5 kJ/mol, respectively. In addition, the overall mass transfer coefficient was measured, and the effect of temperature, concentration, and CO_2 loading was studied. According to them, the overall mass transfer coefficient increased with temperature and K-Tau concentration while it decreased as CO_2 loading increased. The reduction of overall mass transfer coefficient with CO_2 loading is due to a reduction in free taurate molecules available to react with CO_2. K-Tau solution also showed a faster reaction rate with CO_2 at high temperatures in comparison with MEA solution.

In another study, termolecular and zwitterion reaction mechanisms were used by Sodiq et al. (2014) to analyze CO_2 absorption kinetics in sodium salts of proline and taurine solution using the stopped-flow technique. The zwitterion formation was found to be the rate-determining step during reaction with CO_2. They also indicated that N-Pro has a faster reaction rate with CO_2 than N-Tau solution. Portugal et al. (2008) measured CO_2 absorption rate in K-Thr at temperatures from 293 to 313 K using an SCR. It was reported that K-Thr exhibits a faster reaction rate than diethanolamine (DEA) but slower than K-Gly. Kinetic measurement of CO_2 absorption in 0.25–2 M K-Lys and at temperatures of 298–333 was performed by Shen et al. (2016c). The authors demonstrated that K-Lys has a higher chemical reactivity with CO_2 than K-Pro, K-Sar, and MEA solutions. The reaction order was found to be between 1.36 and 1.54 with respect to K-Lys with means zwitterion deprotonation steps are not much faster than the zwitterion formation step.

The CO_2 absorption rate in water-lean solvents was studied by several researchers (Bian et al. 2019; Li and Shen 2019c). For example, the kinetics of CO_2 absorption in K-Pro/water, K-Pro/ethylene glycol, and K-Pro/ethanol systems at temperatures and concentrations ranging from 275 to 285 K and 0.15–2 M, respectively, using an SCR was evaluated by Bian et al. (2019). Their results showed that the overall reaction rate constant at 280 K for K-Pro/ethylene glycol (43,370 s^{-1}) is higher than that of K-Pro/water (9061 s^{-1}) and K-Pro/ethanol (18153 s^{-1}). The reaction orders with respect to K-Pro in water, ethylene glycol, and ethanol solutions were found to be 1.46, 1.89, and 2, respectively.

Song et al. (2012) studied absorption and desorption rate performance of several amino acid salts based on their molecular structure. They categorized amino acids into four groups, including sterically hindered amino acids, poly amino acids, cyclic amino acids, and linear amino acids. They concluded that a slower absorption rate and faster desorption rate can be achieved for linear amino acids with smaller distances between amino and carboxyl groups and bulkier substituted groups. The sterically hindered amino acids also showed a slow absorption rate and high desorption rate due to the bulkier substituent group that exhibited stronger steric repulsion. The presence of carbonyl oxygen in structure of di-amino acids leads to a faster desorption rate and slower absorption rate. Moreover, the slow desorption rate and fast absorption rate were explained due to the protruding structures of the cyclic amino acids.

The Arrhenius curves of the reaction rate constants between CO_2 and different amino acid salts (Aronu et al. 2011b; Guo et al. 2013; Hu et al. 2018; Hwang et al. 2010; Majchrowicz et al. 2014a; Park et al. 2008; Paul and Thomsen 2012; Shen et al. 2013b, 2016b, 2016c; Sodiq et al. 2014; Thee et al. 2014; Wei et al. 2014) are shown in Figure 7.

In addition, a comparison between absorption rate performance of different amino acid salts is necessary in order to better understand the results in the literature. Therefore, the overall reaction rate constant (K_{ov}) (Aronu et al. 2011b; Kim et al. 2012; Kumar et al. 2003b; Paul and Thomsen 2012; Portugal et al. 2008, 2017; Shen et al. 2016c, 2016b; Shen and Yang 2016a; Simons et al. 2010; Ying and Eimer 2013) as a function of amino acid salt concentration at 298.15 and 313.15 K is shown in Figure 8 and Figure 9, respectively. As illustrated in these figures, K-Lys and K-Sar present the fastest reaction kinetics while K-Tau shows the slowest reaction rate among all amino acid salts. Although

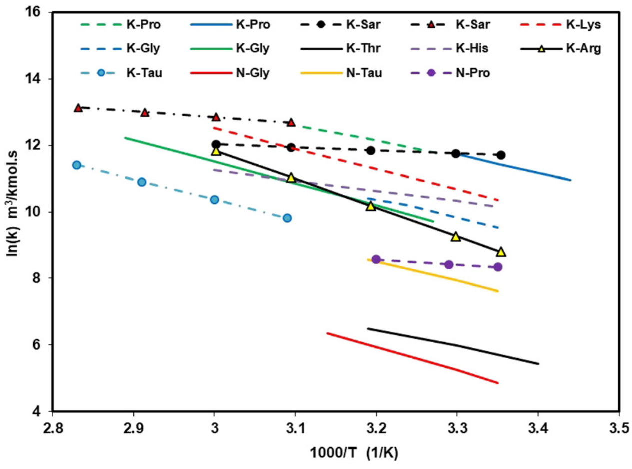

Figure 7: Reaction rate constant expressions for CO_2 reacting with amino acid salt solutions.

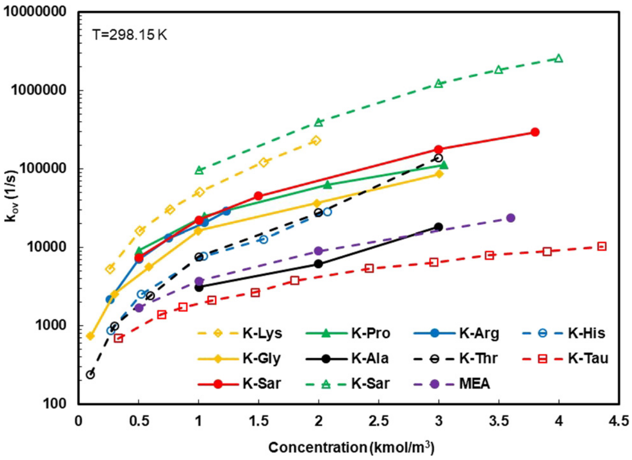

Figure 8: Overall kinetic constants for CO_2 absorption in amino acid salt solutions at 298 K.

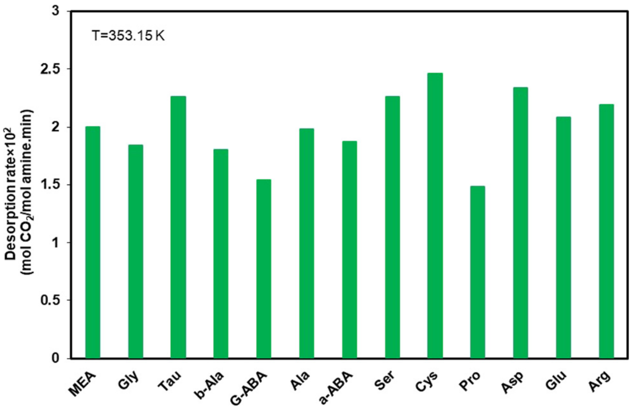

Figure 10: Desorption rate of CO_2 in 1 M potassium salts of different amino acids at 353.15 K. Data from (Song et al. 2012).

K-Pro, K-Arg, and K-Gly indicate a lower absorption rate than K-Lys and K-Sar, their CO_2 absorption rate performance is much better than that of other amino acid salts. K-Arg has a molecular structure similar to primary amines and therefore is expected to have a fast reaction rate. It can also be seen that all amino acid salts except K-Tau and K-Ala have better reactivity with CO_2 than MEA.

Generally, higher desorption rate leads to a lower thermal energy for regeneration of the saturated solvent (Song et al. 2012). Therefore, choosing solvent with fast desorption rate is very important. Song et al. (2012) measured the desorption rate of CO_2 into potassium salt of several amino acids.

Figure 10 shows CO_2 desorption rate of amino acid salt solutions and MEA at 353.15 K at the same concentration. According to their results, potassium salt of asparagine, taurine, serine, arginine, cysteine, and glutamine showed faster desorption rate than MEA while alanine, *β*-alanine, glycine, proline, *γ*-aminobutyric acid, and *α*-aminobutyric acid displayed slower desorption rate than aqueous MEA solution. The results indicate that K-Cys solution has the highest desorption rate. K-Tau solution, which showed the lowest absorption rate, is one of the best amino acid salts in terms of desorption rate. K-Ser exhibits a similar desorption rate with K-Tau.

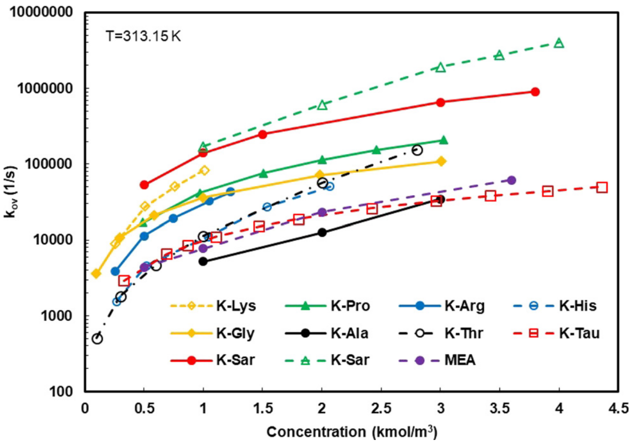

Figure 9: Overall kinetic constants for CO_2 absorption in amino acid salt solutions at 313 K.

Although the K-Pro presented a better performance in terms of absorption rate, its desorption rate was the lowest among investigated amino acid salts. The similar behavior can also be observed for potassium salt of glycine. He et al. (2017) studied the desorption rate performance of potassium salts of three amino acids, including sarcosine, glycine, and taurine at 375.15 K, and compared with 2 kmol/m^3 MEA solution. It was found that K-Tau and K-Sar exhibit the fastest and the lowest desorption rate, respectively. In other words, according to their results, the desorption rate follows the order: K-Tau > MEA > K-Gly > K-Sar.

The results of this section can be summarized as follows:
- The CO_2 absorption rate increases as temperature and concentration increase.
- Smaller distances between amino and carboxyl groups and bulkier substituted groups lead to slower absorption rate and faster desorption rate.
- The sterically hindered amino acid salts show a slow absorption rate and fast desorption rate due to the bulkier substituent group.
- The carbonyl oxygen in di-amino acid structure results in a faster desorption rate and slower absorption rate.
- K-Sar, K-Lys, and K-Pro have fast reactivity with CO_2.
- K-Asp, K-Tau, K-Ser, K-Arg, K-Cys, and K-Glu showed faster desorption rate than MEA.

2.8 Surface tension

High surface tension of amino acids due to their ionic nature is one of the advantages which makes them an attractive absorbent in membrane gas absorption processes because it can avoid pore wetting at the membrane contactor (Song et al. 2012). Since surface tension affects the effective mass transfer area in a packed column, it is necessary to study this parameter at different experimental conditions. Song et al. (2012, 2011) measured surface tension of several amino acid salts using a commercial bubble pressure meter at a temperature and concentration of 298.15 K and 2.5 M, respectively. In addition, they added piperazine (PZ) to K-Ala and K-Ser and found that the addition of PZ to amino acid salts decreases their surface tension. Lee et al. (2005) determined surface tension of 10–50 wt% N-Gly solution using an automated tensiometer. The results showed that surface tension increases with a rise in concentration of amino acid salt. Surface tension of potassium salts of glycine, sarcosine, and taurine at 298.15 K was investigated by Park et al. (2014). Their results showed that these three amino acid salts have higher surface tension than MEA. They also studied the effect of addition of PZ to taurine and glycine and observed that surface tension decreases with the addition of piperazine to amino acid salts.

He et al. (2017) reported the surface tension of some amino acid salts at temperatures of 298, 313, 328, and 343 K and concentration of 1 M. According to their results, surface tension of potassium salts of proline, glycine, arginine, and sarcosine decreases as temperatures increases from 298 to 343 K. The surface tension of 5–25 wt% potassium salt of phenylalanine at temperatures of 298–343 K was determined by Garg et al. (2016b). They observed higher values of surface tension for K-Phe when concentration increases from 5wt% to 25 wt%. This effect can be explained by the fact that hydroxyl ions in amino acid salt solution cause the stability of the surface tension to increase with increasing concentration.

A comparison between surface tension of amino acid salts with water and MEA solution is presented in Figure 11. The results demonstrated that K-Gly and K-Pro have the highest and lowest surface tension among amino acid salts, respectively. Although the surface tension of K-Tau and K-Ala is lower than that of K-Gly, they showed good performance when compared with other amino acid salts. It can also be observed that potassium salts of glycine, taurine, alanine, threonine, and sarcosine have higher surface tension than water while the surface tension of arginine, phenylalanine, and proline was found to be lower than that of water.

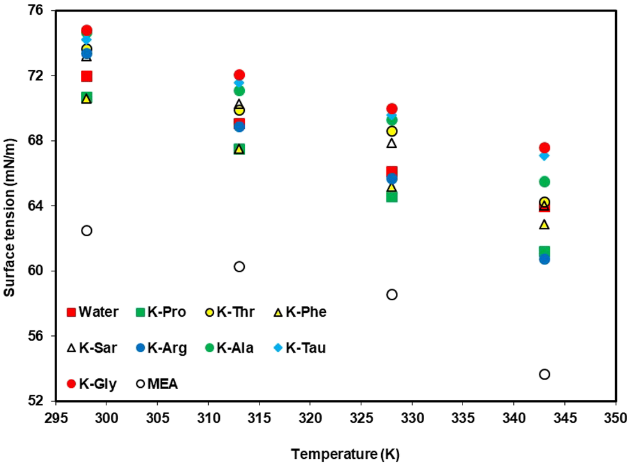

Figure 11: Comparison of surface tension of 1 M amino acid salt solutions with MEA and water. Data from (Garg et al. 2016b; He et al. 2017; Song et al. 2012).

In addition, Figure 11 demonstrates that temperature has a negative effect on surface tension. Molecules of water and amino acid salts tend to move apart at high temperature, which causes a weakening of hydrogen bonding. Therefore, surface tension decreases with temperature which can help in finding a suitable absorbent with high surface tension performance at high temperature for the gas absorption process.

The important conclusions of this section are as follows:

- The surface tension of amino acid salts increases as concentration increases.
- The temperature has a negative effect on surface tension of amino acid salts.
- Amino acid salts are better choice than MEA for using in membrane contactors from the surface tension point of view.
- Amino acid salts have much higher surface tension than MEA.
- K-Gly has the highest surface tension among amino acid salts.

2.9 Heat of CO_2 absorption

The greatest challenge in CO_2 capture using MEA solution is high energy consumption during regeneration of solvent (Svendsen et al. 2011). The reason is that MEA solution as a primary alkanolamine reacts with CO_2 and forms primary stable carbamate which needs high energy for regeneration. Therefore, an important requirement of a CO_2 chemical absorbent is a lower energy requirement for regeneration which leads to reducing total operation costs (Majchrowicz and Brilman 2015).

Zhao et al. (2017a) estimated the heat of CO_2 absorption for potassium salt of lysine using the Gibbs-Helmholtz equation and concluded that 20–30 wt% K-Lys exhibits a lower absorption heat (55–70 kJ/mol) in comparison with 30 wt% MEA solution (84.5 kJ/mol). In another study (Zhao et al. 2017b), they determined the absorption heat for 32 wt % K-Lys solution at different values of CO_2 loading using a calorimeter. They found that the heat of CO_2 absorption decreases with increasing CO_2 loading capacity and reaches an absorption heat of about 60 kJ/mol at CO_2 loading equal to 1.2 (mol CO_2/mol solvent). This result can be explained mainly due to the fact that at high CO_2 loading, physical absorption dominates, and bicarbonate is formed that leads to a reduction in heat of CO_2 absorption.

Aronu et al. (2011a) calculated absorption heat of 3.5 M potassium salt of sarcosine at CO_2 loading of 0.2 (mol CO_2/mol solvent) and compared it with 30 wt% MEA solution at the same CO_2 loading capacity. According to their work, K-Sar showed absorption heat of 66.7 kJ/mol which is less than that of MEA with absorption heat of 84.5 kJ/mol. Majchrowicz and Brilman (2012) measured CO_2 solubility of 0.5 M K-Pro and determined its heat of absorption at CO_2 loading of 0.8 (mol CO_2/mol solvent) using experimental solubility data and the Gibbs-Helmholtz equation. Absorption heat of CO_2 was found to be 54.3 kJ/mol.

Salazar et al. (2010) investigated performance of 10 wt % N-Gly solution in terms of absorption heat using a calorimeter and observed N-Gly with absorption heat of 72.5 kJ/mol has a better performance than MEA in terms of absorption heat.

A differential reaction calorimeter was used by Lim et al. (2012) in order to study absorption heat of 2.5 M K-Pro and 2.5 M K-Ala at temperatures of 298 and 313 K. They reported that absorption heat at 298 K was found to be 53.26 and 90.2 kJ/mol for K-Ala and K-Pro while at 313 K, absorption heat was found to be 66.13 and 86.17 kJ/mol for K-Ala and K-Pro, respectively. Based on their results, K-Ala solution as a sterically hindered amino acid salt offers lower absorption heat in comparison with K-Pro that can be explained due to unstable carbamate formation.

The summary of this section is as follows:

- Stable carbamate formation during reaction needs high regeneration energy.
- The heat of CO_2 absorption decreases with increasing CO_2 loading capacity.
- Bicarbonate formation leads to a reduction in heat of CO_2 absorption.
- Sterically hindered amino acid salts offer low absorption heat due to unstable carbamate formation.
- K-Ala, K-Sar, and K-Pro present lower absorption heat than MEA.

2.10 Precipitation

Although amino acid salts present many advantages, they also have their own limitations. Amino acid salts precipitate at high concentrations or high CO_2 loading during CO_2 absorption which causes damage to absorption plant and also reduces mass transfer (Aronu et al. 2011c). However, low concentration of amino acid salts does not produce precipitates.

Aronu et al. (2014), Majchrowicz et al. (2009), and Rabensteiner et al. (2015) showed that precipitation occurs at concentrations higher than 3.5 M for K-Sar, 3 M for K-Pro, and 30 wt% for K-Gly, respectively. Aronu et al. (2014) in another work reported that energy requirement for desorption in a precipitating K-Sar system is lower than nonprecipitating K-Sar system and lower than MEA solution. Majchrowicz et al. (2009) found that the precipitate composition depends on the type of amino acid salt. They explained that the precipitation can consist in the form of protonated taurine for K-Tau system and bicarbonate salt for K-Sar, K-Ala, and K-Pro systems. The different compositions of the solid particles can affect desorption performance and thus CO_2 capture efficiency (Majchrowicz 2014b). In addition, it was found that lithium salt of amino acids precipitates more easily than potassium and sodium salts of amino acids.

In another study, Majchrowicz and Brilman (2012) observed an increase in CO_2 loading capacity of 3 M K-Pro as a result of precipitation at 285 K. The greater CO_2 loading may also offer a possibility of lower regeneration energy requirement for amino acid salts. Moreover, at high CO_2 loading capacity, driving force is high due to the precipitation; therefore, an increase in absorption kinetics can be expected (Majchrowicz 2014b). Aronu et al. (2013) observed an increase in absorption rate of CO_2 in potassium salts of sarcosine, alanine, and serine due to the precipitation. The same finding was obtained in 4 M potassium taurate by Sanchez-Fernandez (2013a). Ma (2014) found that the precipitation has a positive effect on absorption rate of potassium salt of alanine, while no effect of precipitation was observed for sodium salt of alanine.

Kumar et al. (2003a, 2002) studied the effect of precipitation on CO_2 loading capacity of K-Tau at temperatures of 298.15–313.15 K. According to their results, the precipitation starts at CO_2 loadings higher than 0.35, 0.4, and 0.5 (mol CO_2/mol amine) for 3, 4, and 2 M K-Tau solution, respectively. They also found that crystallization of the reaction product has a positive effect of CO_2 loading capacity of K-Tau. For example, the CO_2 loading capacity of 3 M K-Tau solution was observed to be increased by 40% due to the precipitation. This effect can be explained by the fact that crystallization of the amino acid salts decreases their concentration in the solution, which shifts the reactions towards the formation of more products resulting in higher CO_2 loading.

In another study, Kumar et al. (2003c) investigated the effect of CO_2 loading capacity on mass transfer coefficient in the absence and presence of precipitation for K-Tau. It was concluded that the effect of solid particles of the reaction product on the mass transfer coefficient in the precipitation region is significant. The precipitation of K-Tau leads to a reduction in mass transfer coefficient by 15% while in the nonprecipitation region, this reduction is about 2%. In addition, their results revealed that the crystallizing reaction product is the protonated taurine which is in good agreement with findings by Majchrowicz et al. (2009).

The precipitation behavior of several amino acid salts was studied by Lerche et al. (2012). It was reported that precipitation composition for K-Gly and K-Lys was a mixture of the zwitterion form of amino acid and potassium bicarbonate. According to their results, K-Lys has very little tendency to form precipitation in comparison to K-Gly, K-Pro, and K-Tau.

Song et al. (2011) and Mazinani et al. (2015) observed no precipitation during CO_2 absorption for 41 wt% K-Lys and 14.3 wt% K-Ser, respectively.

Sanchez-Fernandez (2013a,b) proposed a new CO_2 absorption process based on precipitation of K-Tau. The energy requirement for regeneration was found to be 2.4 2.4 GJ/tCO_2 for 4 M K-Tau which shows 35% reduction in comparison with 5 M MEA (3.7 GJ/tCO_2). In another study (Sanchez-Fernandez et al. 2014), it was concluded that K-Ala has even better desorption performance than K-Tau due to the lower heat of dissolution of alanine. The precipitation of amino acid salts occurs at high CO_2 loading capacity due to decrease in pH of solution. This decrease in pH during solvent regeneration would help to reduce energy consumption for regeneration. The precipitate type for K-Ala was also found to be potassium bicarbonate.

In recent years, CO_2 absorption performance in nonaqueous amino acid salt systems was studied by several researchers (Alivand et al. 2019; Bian and Shen 2018; Guo et al. 2018; Li et al. 2018, 2019b; Shen et al. 2017b). For example, Shen et al. (2017b) and Bian and Shen (2018) showed that the precipitation contains proline salt and bicarbonate for K-Pro/ethanol system. Their results indicated that 55–60% of CO_2 is absorbed in the solid phase. Moreover, it was revealed that the CO_2 absorption rate increases in the precipitation region due to a rise in driving force. The authors also concluded that endothermic enthalpy of precipitation for K-Pro/ethanol solution could save the energy required for CO_2 absorption process.

In a similar work, Guo et al. (2018) observed a slow process for precipitation formation in K-Lys/ethanol system. Alivand et al. (2019) proposed K-Gly/DMF/H_2O system for CO_2 absorption and observed that liquid phase was free from bicarbonate and carbamate.

The summary of this section is as follows:

- Amino acid salts precipitate at high concentrations or high CO_2 loading capacity.
- The lithium salt of amino acids precipitates more easily than potassium or sodium salts.
- The precipitation can consist in the form of protonated amino acid, bicarbonate salt of amino acid.
- The energy requirement for regeneration is lower in a precipitating amino acid salt system.
- The crystallization of the reaction product leads to an increase in CO_2 loading capacity.
- The precipitation has a positive effect on absorption rate of some amino acid salt solutions.
- K-Lys has very little tendency to form precipitation compared to K-Gly, K-Pro, and K-Tau.

2.11 Toxicity

The toxicity of amines is another challenge for CO_2 capture which needs to be addressed for reliable practical application. Since a solvent with high toxicity is not a suitable choice for the CO_2 absorption process, the environmental issues associated with absorbents should be studied. Performance of different amino acids was compared with PZ, MEA, MDEA, DEA, and AMP as widely studied solvents in the literature in this section.

Figure 12 presents the lethal dose (LD_{50}) of various amino acids. The LD_{50} is defined as the amount of a toxic material which causes the death of 50% of a group of tested animals in a certain time (Shariff and Shaikh 2017). Data presented in this are figure taken from (15 May 2020, Fishersci.com/store/msds, Sigmaaldrich.com, Spectrumrx.com/msds, Sciencelab.com/msds, Lewisu.edu/academics/biologgy, Cir-safety.org/sites, Perkinelmer.com, Pubchem.ncbi.nlm.nih.gov/compound, Cdhfinechemical.com/images/product/msds). According to this definition, higher LD_{50} indicates a lower toxicity. It can be seen that all amino acids have less toxicity in comparison with amines, including MDEA, AMP, DEA, MEA, and PZ. Among the amines investigated, MDEA as a tertiary amine showed the

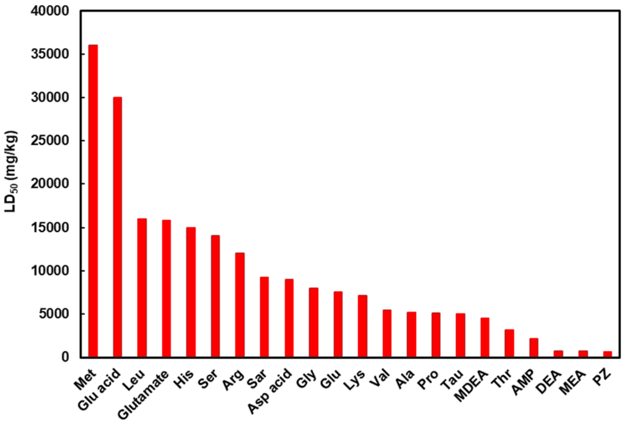

Figure 12: A comparison between toxicity of various amino acid salts with amines.

lowest toxicity, while PZ as a cyclic amine offers the highest toxicity. However, MDEA exhibits more toxicity than all amino acids except threonine. AMP (hindered amine) indicated the higher toxicity than amino acids and MDEA, but its toxicity is still better than MEA (primary amine), PZ, and DEA (secondary amine). A comparison between the toxicity of the amino acids showed that methionine and threonine with LD_{50} values of equal to 36,000 and 3098 mg/kg have the lowest and the highest toxicity, respectively. From the above comparison, it was found that amino acids have much lower toxicity than amine solutions and thus can be considered as environmentally friendly solvents.

2.12 Solvent degradation

Thermal and oxidative degradation are important issues in gas absorption from flue gases because they cause solvent loss, environmental problems, and increased corrosion rate (Fytianos et al. 2016).

Zhao et al. (2017b) investigated thermal and oxidative degradation of potassium salt of lysine at 383 and 423 K under static N_2 and O_2 exposure conditions for 15 days. They concluded that K-Lys has high resistance to thermal degradation and less solvent loss than MEA solution. The degradation products were found to be 6-amino-2-oxohexanoate, 5-aminopentanamide, lysine dimmer, and 2-amino-hexano-6-lactam.

Similar results were observed by Li et al. (2019d). They studied thermal degradation of K-Lys solution in the presence of CO_2 for temperatures between 383 and 423 K. It was found that K-Lys presents better resistance to thermal degradation in comparison with K-Gly, K-Sar, and MEA solutions. They also concluded that alkalinity of solution decreased by 3% at 423 K in the presence of CO_2. Moreover, lysine dimmer and 2-amino-hexano-6-lactam were reported as degradation products.

Aldenkamp et al. (2014) investigated degradation performance of K-Gly solution and observed a significant degradation for K-Gly solution at 393 K. Huang et al. (2013) evaluated thermal degradation of several amino acid salt solutions, including N-Sar, N-Gly, and N-Ala at temperatures up to 418 K. Their results revealed that the amino acid salts tested have faster degradation rate in comparison with MEA solution. They also concluded that sodium salts of sarcosine and alanine present the slowest and fastest degradation rates, respectively. Moreover, thermal degradation products for N-Ala were tetrahydro-1,3-oxazin-6-one, Ala-dimer carbamate, and Ala dimer.

Epp et al. (2011) measured oxidative degradation of K-Gly solution and found that K-Gly shows less resistance to oxidative degradation when compared to MEA. Based on their observation, formaldehyde, amides, and ammonia were reported as oxidative degradation products. Moioli et al. (2019) compared the performance of K-Tau as a solvent with MEA and observed much lower degradation rate for K-Tau in comparison with MEA. Studies on the degradation of amino acid salts during CO_2 absorption are rare in the literature, and thus, more experiments on the degradation of amino acid salts are necessary to make a better judgment about them.

The key messages of this section are as follows:

- Steric hindrance at the amine group protects the amino acid against degradation.
- An amino acid salt with longer chain between the amine and carboxylate has faster degradation rate.
- K-Lys has high resistance to thermal degradation and less solvent loss than K-Gly, K-Sar, and MEA.
- N-Sar, N-Gly, and N-Ala showed faster thermal degradation than MEA.
- K-Gly presents less resistance to oxidative degradation compared to MEA.

2.13 Corrosion rate

Corrosion is a serious problem in gas absorption units because it reduces the equipment life and thus increases capital costs (Shaikh et al. 2013). Since amino acid salt solutions are still new absorbents for CO_2 capture, investigation and experimental data on corrosion rate of amino acid salts are very scarce in the literature. The corrosion rate experiments of MDEA + arginine solution were carried out by Talkhan et al. (2019) at a temperature range 293–323 K using a three-electrode electrochemical glass cell. The results indicated that addition of arginine to MDEA decreases the corrosion rate. This trend can be explained by the inhibition effect of arginine. Arginine as an amino acid acts as an inhibitor and reduces the corrosion rate of MDEA.

Mazinani et al. (2015) measured corrosion rate of K-Lys solution without dissolved CO_2 at concentrations of 0.5, 1.5, and 2.5 M using an electrochemical technique. It was reported that the corrosion rate increases from 0.0008 to 0.012 mm/yr as concentration of K-Lys increases from 0.5 to 2.5 M. In another study (Mazinani et al. 2011), they proposed a blend solution of N-Gly + MEA as a solvent and evaluated its corrosion rate at 308 K. According to their findings, the addition of N-Gly to MEA accelerates the corrosion rate. Ramazani et al. (2016) reported a corrosion rate of K-Lys + MEA solution at 313.15 K. Their results showed that K-Lys + MEA exhibits a higher corrosion rate at high mole fraction of K-Lys in a blend solution. The amount of bicarbonate ion in solution increases when K-Lys is added, which resulted in an increase in corrosion rate.

Ahn et al. (2010) determined the corrosion rate of K-Gly and K-Tau solutions and studied the effect of temperature, CO_2 loading capacity, and concentration on corrosion rate. They concluded that with an increasing concentration of amino acid salt, the corrosion rate of K-Tau increases while the corrosion rate of K-Gly decreases. Potassium salt of taurine indicated a lower corrosion rate when compared to MEA. In addition, they observed the fastest corrosion rate at high temperature and CO_2 loading capacity. The negative and positive effect of amino acid salts on corrosion rate shows that more investigation on corrosion behavior of amino acid salts is still required.

3 Blend of amino acid salts and amines

In recent years, the use of different types of amino acid salt solutions mixed with other absorbents such as amines and inorganic solvents to form new solvents has drawn attention. Several researchers investigated performance of amino acid salts as a promoter to be added to other absorbents such as potassium carbonate (K_2CO_3), trisodium phosphate, and MDEA to improve CO_2 absorption rate (Benamor et al. 2016; Lee et al. 2015; Li et al. 2019a; Ramezani et al. 2017a,b, 2018a,b, 2019; Shen et al. 2013a,b; Xiang et al. 2013; Yang et al. 2014b; Yoo et al. 2018).

Hu et al. (2017a) studied the effect of addition of potassium salts of lysine, leucine, glycine, sarcosine, and proline on CO2 absorption rate of K_2CO_3. They discovered that K-Pro and K-Sar have better performance to improve absorption rate of CO_2 in K_2CO_3 solution compared to K-Lys, K-Gly, and K-Leu. Moreover, their results showed that K_2CO_3 + K-Sar and K_2CO_3 + K-Pro exhibit faster absorption rate than K_2CO_3 + MEA solution. Shen et al. (2013a) measured CO_2 desorption rate of K_2CO_3 solution promoted by arginine. The findings of the study showed that the addition of arginine to K_2CO_3 can increase CO_2 desorption rate, which leads to less energy consumption for the regeneration of saturated solvent.

The kinetics of CO_2 absorption in Gly + MDEA solution at temperature ranging from 293 to 313 K using a stopped-flow technique was investigated by Benamor et al. (2016). This study showed that the reaction rate constant increases with increasing glycine concentration in the solution. Mondal and Samanta (2019) determined kinetics data and CO_2 loading capacity of hexamethylenediamine (HMDA) blended with sodium glycinate solution at temperatures of 298–333 K. It was concluded that blended solution of HMDA + N-Gly presents better absorption and kinetics characteristics than N-Gly.

The CO_2 cyclic capacity of K_2CO_3 blended with three amino acid salts was investigated by Li et al. (2019a) at absorption and desorption temperatures of 313.15 and 353.15 K, respectively. They concluded that that K_2CO_3 + amino acid salts have higher CO_2 cyclic capacity than MEA solution. Moreover, higher cyclic capacity was found for K_2CO_3 + K-Arg (α_{cyc} = 0.678) compared to K_2CO_3 + K-Gly (α_{cyc} = 0.57) and K_2CO_3 + K-Lys (α_{cyc} = 0.67). Song et al. (2012) observed that K-Ala + PZ and K-Ser + PZ present faster desorption rate and higher cyclic capacity than single K-Ala and K-Ser. In a similar work, Park et al. (2014) showed that blend of K-Tau and PZ exhibits higher cyclic capacity (α_{cyc} = 0.122) than K-Tau (α_{cyc} = 0.108).

Mazinani et al. (2011) measured CO_2 loading capacity and corrosion rate of MEA blended with N-Gly for temperatures between 298 and 313 K at low CO_2 partial pressures. It was reported that enhancing N-Gly concentration in the blend solution has been led to an increase in CO_2 loading capacity and corrosion rate. In addition, the authors compared CO_2 loading capacity of MEA + N-Gly solution with MEA at 298 K and observed that MEA + N-Gly has higher CO_2 loading capacity than MEA at CO_2 partial pressures higher than 15 kPa. Likewise, Ramazani et al. (2016) investigated CO_2 absorption in MEA + K-Lys system at temperatures 303–323 K using an SCR. According to their results, CO_2 loading and corrosion rate increase when concentration of K-Lys increases in the solution.

Hamzehie and Najibi (2016) proposed a blend of AMP and K-Pro and evaluated its absorption performance in presence of oxygen. It was observed that decrease in CO_2 loading capacity of AMP + K-Pro solution, due to amine degradation in presence of oxygen, is much lower than single AMP solution. Blend of potassium salts of alanine and serine with PZ was used by Kang et al. (2013). According to their results, K-Ala + PZ has higher CO_2 loading than K-Ser + PZ. Lu et al. (2011) measured surface tension of K-Gly and K-Gly + PZ solutions at 288 K. The results revealed that the addition of PZ to K-Gly has a negative effect on surface tension since the surface tension decreased from 76.1 to 73.5 (mN/m) when PZ was added.

4 Conclusions

In this review, the CO_2 absorption characteristics of 20 common amino acid salts were screened. It was found that potassium salt of amino acids has greater CO_2 loading capacity than sodium salt. K-Lys, K-Gly, K-His, and K-Glu exhibited higher CO_2 loading capacity than other amino acid salts and MEA. From the cyclic capacity point of view, K-Arg, K-Ser, K-Asp, K-ABA, K-Ala, and K-Glu might be better choices than MEA. Moreover, the viscosity of amino acid salts showed a strong function of temperature and concentration. Most amino acid salts offer a greater pKa than MEA, which shows their high reactivity with CO_2. Smaller distances between amino and carboxyl groups and bulkier substituted groups lead to slower absorption rate, faster desorption rate, and greater cyclic capacity. K-Asp, K-Tau, K-Ser, K-Arg, and K-Cys indicated fast desorption rate while high absorption rate was observed for K-Sar, K-Lys, and K-Pro. Amino acid salts have much higher surface tension than MEA which makes them favorable candidates for CO_2 absorption in membrane contactors. Bicarbonate or unstable carbamate formation has positive effect on regeneration energy requirement of amino acid salts. K-Ala, K-Sar, K-Lys, and K-Pro are attractive candidates for CO_2 capture from the perspective of CO_2 absorption heat. From toxicity analysis, amino acids have much lower toxicity than amines such as MDEA, AMP, DEA, MEA, and PZ and thus can be considered as environmentally friendly solvents. Since studies on the corrosion rate and degradation of amino acid salts during CO_2 absorption are rare in the literature, more investigation is necessary to make a better judgment about them. The precipitation formation of amino acid salts could have positive effects such as lower regeneration energy requirement and higher CO_2 loading capacity if well controlled. The lithium salt of amino acids was reported to be precipitated more easily than their potassium or sodium salts. The CO_2 absorption performance of amino acid salts can be improved by blending with various amines. Based on the study carried out in this review work, K-Sar, K-Lys, and K-Pro have the potential to be considered as attractive candidates for CO_2 absorption. K-Sar could be used as an effective solvent for CO_2 capture at high temperatures. For future work, extensive studies on the corrosion rate, degradation, precipitation, and regeneration energy of amino acid salts would be helpful for efficient solvent screening.

Abbreviations

AMPD	2-amino-2-methyl-1,3-propanediol
AMP	2-amino-2-methyl-1-propanol
Asp acid	Aspartic acid
CO_2	Carbon dioxide
DEA	Diethanolamine
Glu acid	Glutamic acid
HMDA	Hexamethylenediamine
Iso	Isoleucine
K_2CO_3	Potassium carbonate
KOH	Potassium hydroxide
K-Arg	Potassium salt of arginine
K-ABA	Potassium aminobutyrate
K-Asp	Potassium salt of asparagine
K-Gly	Potassium glycinate
K-Glu	Potassium salt of glutamine
K-His	Potassium salt of histidine
K-Phe	Potassium salt phenylalanine
K-Pro	Potassium prolinate
K-Sar	Potassium sarcosinate
K-Ser	Potassium serinate
K-Thr	Potassium threonate
K-Tau	Potassium taurate
K-Met	Potassium salt of methionine
K-Lys	Potassium lysinate
Leu	Leucine
MEA	Monoethanolamine
MDEA	Methyldiethanolamine
N-Ala	Sodium alaninate
N-Gly	Sodium glycinate
PZ	Piperazine
Thr	Threonine
Try	Tryptophan
TIPA	Triisopropanolamine
b-Ala	b-alanine
G-ABA	γ-aminobutyric acid
α-ABA	α-aminobutyric acid

Author contribution: All the authors have accepted responsibility for the entire content of this submitted manuscript and approved submission.

Research funding: None declared.

Conflict of interest statement: The authors declare no conflicts of interest regarding this article.

References

Aftab, A., Shariff, A., Garg, S., Lal, B., Shaikh, M., and Faiqa, N. (2018). Solubility of CO_2 in aqueous sodium alaninate: experimental study and modeling using Kent Eisenberg model. Chem. Eng. Res. Des. 131: 385–392.

Ahn, S., Song, H., Park, J., Lee, J., Lee, I., and Jang, K. (2010). Characterization of metal corrosion by aqueous amino acid salts for the capture of CO_2. Korean J. Chem. Eng. 27: 1576–1580.

Aldenkamp, N., Huttenhuis, P., Elk, N., and Hamborg, E. (2014). Solubility of carbon dioxide in aqueous potassium salts of glycine and taurine at absorber and desorber conditions. J. Chem. Eng. Data 59: 3397–3406.

Alivand, M., Mazaheri, O., Wu, Y., Stevens, G., Scholes, C., and Mumford, K. (2019). Development of aqueous-based phase change amino acid solvents for energy-efficient CO_2 capture: the role of antisolvent. Appl. Energy 256: 113911.

Aronu, U.E., Svendsen, H., and Hoff, K. (2010). Investigation of amine amino acid salts for carbon dioxide absorption. Int. J. Greenh. Gas Con. 4: 771–775.

Aronu, U.E., Hessen, E., Warberg, T., Hoff, K., and Svendsen, H. (2011a). Vapor–liquid equilibrium in amino acid salt system: experiments and modeling. Chem. Eng. Sci. 66: 2191–2198.

Aronu, U.E., Hartono, A., Hoff, K., and Svendsen, H. (2011b). Kinetics of carbon dioxide absorption into aqueous amino acid salt: potassium salt of sarcosine solution. Ind. Eng. Chem. Res. 50: 10465–10475.

Aronu, U.E., Hoff, K., and Svendsen, H. (2011c). Vapor–liquid equilibrium in aqueous amine amino acid salt solution: 3-(methylamino)propylamine/sarcosine. Chem. Eng. Sci. 66: 3859–3867.

Aronu, U.E., Hartono, A., and Svendsen, H. (2012). Density, viscosity, and N_2O solubility of aqueous amino acid salt and amine amino acid salt solutions. J. Chem. Thermodyn. 45: 90–99.

Aronu, U.E., Ciftja, A., Kim, I., and Hartono, A. (2013). Understanding precipitation in amino acid salt systems at process conditions. Energy Procedia 37: 233–240.

Aronu, U.E., Kim, I., and Haugen, G. (2014). Evaluation of energetic benefit for solid-liquid phase change CO_2 absorbents. Energy Procedia 63: 532–541.

Benamor, A., Al-Marri, M., Khraisheh, M., and Nasser, M. (2016). Reaction kinetics of carbon dioxide in aqueous blends of methyldiethanolamine and glycine using the stopped flow technique. J. Nat. Gas Sci. Eng. 33: 186–195.

Bernhardsen, I., and Knuutila, H. (2017). A review of potential amine solvents for CO_2 absorption process: absorption capacity, cyclic capacity, and pKa. Int. J. Greenh. Gas Con. 61: 27–48.

Bian, Y., and Shen, S. (2018). CO_2 ab.sorption into a phase change absorbent: water-lean potassium prolinate/ethanol solution. Chin. J. Chem. Eng. 26: 2318–2326.

Bian, Y., Shen, S., Zhao, Y., and Yang, Y. (2016). Physicochemical properties of aqueous potassium salts of basic amino acids as absorbents for CO_2 Capture. J. Chem. Eng. Data 61: 2391–2398.

Bian, Y., Zhao, Y., and Shen, S. (2017). Characteristics of potassium prolinate + water + ethanol solution as a phase changing absorbent for CO_2 capture. J. Chem. Eng. Data 62: 3169–3177.

Bian, Y., Li, H., and Shen, S. (2019). Reaction kinetics of carbon dioxide with potassium prolinate in water-lean solvents. Chem. Eng. Sci. 199: 220–230.

Chang, Y., Leron, R., and Li, M. (2015). Carbon dioxide solubility in aqueous potassium salt solutions of L-proline and aminobutyric acid at high pressures. J. Chem. Thermodyn. 83: 110–116.

Chen, C.C., and Evans, L. (1986). A local composition model for the excess Gibbs energy of aqueous electrolyte systems. AIChE J. 32: 444–454.

Chen, C.C., Britt, H., Boston, J., and Evans, L.B. (1979). Extension and application of the Pitzer equation for vapor-liquid equilibrium of aqueous electrolyte systems with molecular solutes. AIChE J. 25: 820–831.

Chen, C.C., Britt, H., Boston, J., and Evans, L.B. (1982). Local composition model for excess Gibbs energy of electrolyte systems. Part I: single solvent, single completely dissociated electrolyte systems. AIChE J. 28: 588–596.

Chen, Z.W., Leron, R.B., and Li, M.H. (2015). Equilibrium solubility of carbon dioxide in aqueous potassium L-asparaginate and potassium L-glutaminate solutions. Fluid Phase Equil. 400: 20–26.

Epp, B., Hans, F., and Monika, V. (2011). Degradation of solutions of monoethanolamine, diglycolamine and potassium glycinate in view of tail-end CO_2 absorption. Energy Procedia 4: 75–80.

Franca, R., and Azapagic, A. (2015). Carbon capture, storage, and utilisation technologies: a critical analysis and comparison of their life cycle environmental impacts. J. CO2 Util. 9: 82–102.

Fytianos, G., Seniz, U., Grimstvedt, A., and Hyldbakk, A. (2016). Svendsen, Knuutila H. Corrosion and degradation in MEA based post-combustion CO_2 capture. Int. J. Greenh. Gas Con. 46: 48–56, Available at: https://www.sciencedirect.com/science/article/abs/pii/S1750583615301730-!H.

Garcia, A., Leron, R., Soriano, A., and Li, M. (2015). Thermophysical property characterization of aqueous amino acid salt solutions containing a-aminobutyric acid. J. Chem. Thermodyn. 81: 136–142.

Garg, S., Shariff, A., Shaikh, M., Lal, B., and Aftab, A. (2016a). VLE of CO_2 in aqueous potassium salt of L-phenylalanine: experimental data and modeling using modified Kent-Eisenberg model. J. Nat. Gas Sci. Eng. 34: 864–872.

Garg, S., Shariff, A., Shaikh, M., Lal, B., Aftab, A., and Faiqa, N. (2016b). Selected physical properties of aqueous potassium salt of l-phenylalanine as a solvent for CO_2 capture. Chem. Eng. Res. Des. 113: 169–181.

Garg, S., Shariff, A., Shaikh, M., and Lal, B. (2017a). Experimental data, thermodynamic and neural network modeling of CO_2 solubility in aqueous sodium salt of L-phenylalanine. J. CO2 Util. 19: 146–156.

Garg, S., Murshid, G., Mjalli, F., Ali, A., and Ahmad, W. (2017b). Experimental and correlation study of selected physical properties of aqueous blends of potassium sarcosinate and 2-piperidineethanol as a solvent for CO_2 capture. Chem. Eng. Res. Des. 118: 121–130.

Guo, D., Thee, H., Tan, G., Chen, J., Fei, W., Kentish, S., Stevens, G., and Silva, G. (2013). Amino acids as carbon capture solvents: chemical kinetics and mechanism of the glycine + CO_2 reaction. Energy Fuels 27: 3898–3904.

Guo, H., Li, H., and Shen, S. (2018). CO_2 capture by water-lean amino acid salts: absorption performance and mechanism. Energy Fuels 32: 6943–6954.

Hairul, N., Shariff, A., Tay, W., Mortel, A., Lau, K., and Tan, L. (2016). Modelling of high-pressure CO_2 absorption using PZ + AMP blended solution in a packed absorption column. Sep. Purif. Technol. 165: 179–189.

Hamborg, E., Niederer, J., and Versteeg, G. (2007). Dissociation constants and thermodynamic properties of amino acids used in CO_2 absorption from (293 to 353) K. J. Chem. Eng. Data 52: 2491–2502.

Hamzehie, M., and Najibi, H. (2016). CO_2 solubility in aqueous solutions of potassium prolinate and (potassium prolinate + 2-amino-2-methyl-1-propanol) as new absorbents. J. Nat. Gas Sci. Eng. 34: 356–365.

Harris, F., Kurnia, K., Mutalib, M., and Thanapalan, M. (2009). Solubilities of carbon dioxide and densities of aqueous sodium glycinate solutions before and after CO_2 absorption. J. Chem. Eng. Data 54: 144–147.

Hartono, A., Orji Mba, E., and Svendsen, H.F. (2014). Physical properties of partially CO_2 loaded aqueous monoethanolamine (MEA). J. Chem. Eng. Data 59: 1808–1816.

He, F., Wang, T., Fang, M., Wang, Z., Yu, H., and Ma, Q. (2017). Screening test of amino acid salts for CO_2 absorption at flue gas temperature in a membrane contactor. Energy Fuels 31: 770–777.

Holst, J., Kersten, S., and Hogendoorn, A. (2008). Physiochemical properties of several aqueous potassium amino acid salts. J. Chem. Eng. Data 53: 1286–1291.

Holst, J., Versteeg, G., Brilman, D., and Hogendoorn, J. (2009). Kinetic study of CO_2 with various amino acid salts in aqueous solution. Chem. Eng. Sci. 64: 59–68.

Hu, W., and Chakma, A. (1990). Modelling of equilibrium solubility of CO_2 and H_2S in aqueous diglycolamine (DGA) solutions. Can. J. Chem. Eng. 68: 523–525.

Hu, G., Nicholas, N., Smith, K., Mumford, K., Kentish, S., and Stevens, G. (2016). Carbon dioxide absorption into promoted potassium carbonate solutions: a review. Int. J. Greenh. Gas Con. 53: 28–40.

Hu, G., Smith, K., Wu, Y., Kentish, S., and Stevens, G. (2017a). Screening amino acid salts as rate promoters in potassium carbonate solvent for carbon dioxide absorption. Energy Fuels 31: 4280–4286.

Hu, G., Smith, K., Liu, L., Kentish, S., and Stevens, G. (2017b). Reaction kinetics and mechanism between histidine and carbon dioxide. Chem. Eng. J. 307: 56–62.

Hu, G., Smith, K., Wu, Y., Mumford, K., Kentish, S., and Stevens, G. (2018). Carbon dioxide capture by solvent absorption using amino acids: a review. Chin. J. Chem. Eng. 26: 2229–2237.

Huang, Q., Bhatnagar, S., Remias, J., Selegue, J., and Liu, K. (2013). Thermal degradation of amino acid salts in CO_2 capture. Int. J. Greenh. Gas Con. 19: 243–250.

Hwang, K., Park, D., Oh, K., Kim, S., and Park, S. (2010). Chemical absorption of carbon dioxide into aqueous solution of potassium threonate. Sep. Sci. Technol 45: 497–507.

Jansen, D., Gazzani, M., Manzolini, G., Dijk, E., and Carbo, M. (2015). Pre-combustion CO_2 capture. Int. J. Greenh. Gas Con. 40: 167–187.

Kang, D., Park, S., Jo, H., Min, J., and Park, J. (2013). Solubility of CO_2 in amino-acid-based solutions of (potassium sarcosinate), (potassium alaninate + PZ), and (potassium serinate + PZ). J. Chem. Eng. Data 58: 1787–1791.

Kent, R. and Eisenberg, B. (1976). Better data for amine treating. Hydrocarb. Process 55: 87–90.

Kim, M., Song, H., Lee, M., Jo, H., and Park, J. (2012). Kinetics and steric hindrance effects of carbon dioxide absorption into aqueous potassium alaninate solutions. Ind. Eng. Chem. Res. 51: 2570–2577.

Krupiczka, R., Rotkegel, A., and Ziobrowski, Z. (2015). Comparative study of CO_2 absorption in packed column using imidazolium based ionic liquids and MEA solution. Sep. Purif. Technol. 149: 228–236.

Kumar, P., Hogendoorn, J., Timmer, S., Feron, P., and Versteeg, G. (2003a). Equilibrium solubility of CO_2 in aqueous potassium taurate solutions: Part 2. Experimental VLE data and model. Ind. Eng. Chem. Res. 42: 2841–2852.

Kumar, P., Hogendoorn, J., and Versteeg, G. (2003b). Kinetics of the reaction of CO_2 with aqueous potassium salt of taurine and glycine. AIChE J. 49: 203–213.

Kumar, P., Hogendoorn, J., Feron, P., and Versteeg, G. (2003c). Equilibrium solubility of CO_2 in aqueous potassium taurate solutions: Part 1. crystallization in carbon dioxide loaded aqueous salt solutions of amino acids. Ind. Eng. Chem. Res. 42: 2832–2840.

Kumar, P. (2002). *Development and design of membrane gas absorption processes*, Ph.D. Thesis. Netherlands, University of Twente, Enschede.

Lee, J., Otto, F., and Mather, A. (1976). Equilibrium between carbon dioxide and aqueous monoethanolamine solutions. J. Appl. Chem. Biotechnol. 26: 541–549.

Lee, S., Choi, S., Maken, S., Song, H., Shin, H., Park, J., Jang, K., and Kim, J. (2005). Physical properties of aqueous sodium glycinate solution as an absorbent for carbon dioxide removal. J. Chem. Eng. Data 50: 1773–1776.

Lee, S., Song, H., Maken, S., and Park, J. (2007). Kinetics of CO2 absorption in aqueous sodium glycinate solutions. Ind. Eng. Chem. Res. 46: 1578–1583.

Lee, A., Wolf, M., Kromer, N., Mumford, K., Nicholas, N.J., and Kentish, S. (2015). A study of the vapour-liquid equilibrium of CO_2 in mixed solutions of potassium carbonate and potassium glycinate. Int. J. Greenh. Gas Con. 36: 27–33.

Lerche, B.M., Stenby, E.H., and Thomsen, K. (2012). *CO2 capture from flue gas using amino acid salt solutions*, Ph.D. Thesis. Kgs. Lyngby, Denmark, Technical University of Denmark.

Li, M., and Shen, K. P. (1993). Calculation of equilibrium solubility of carbon dioxide in aqueous mixtures of monoethanolamine and methyldiethanolamine. Fluid Phase Equilib. 85: 129–140.

Li, H., and Shen, S. (2019c). Kinetics of carbon dioxide absorption into water-lean potassium prolinate/ethylene glycol solutions. Ind. Eng. Chem. Res. 58: 9875–9882.

Li, J., Liu, H., Liang, Z., Luo, X., Liao, H., Idem, R., and Tontiwachwuthikul, P. (2015). Experimental study of the kinetics of the homogenous reaction of CO_2 into a novel aqueous 3-diethylamino-1,2-propanediol solution using the stopped-flow technique. Chem. Eng. J. 270: 485–495.

Li, H., Guo, H., Bian, Y., Zhao, Y., and Shen, S. (2018). Measurements and correlations of solubility of N_2O in and density, viscosity of partially CO_2 loaded water-lean amino acid salts. J. Chem. Thermodyn. 126: 82–90.

Li, Y., Wang, L., Tan, Z., Zhang, Z., and Hu, X. (2019a). Experimental studies on carbon dioxide absorption using potassium carbonate solutions with amino acid salts. Sep. Purif. Technol. 219: 47–54.

Li, C., Shi, X., and Shen, S. (2019b). Performance evaluation of newly developed absorbents for solvent-based carbon dioxide capture. Energy Fuels 33: 9032–9039.

Li, C., Zhao, Y., and Shen, S. (2019d). Aqueous potassium lysinate for CO_2 capture: evaluating at desorber conditions. Energy Fuels 33: 10090–10098.

Liang, Z., Fu, K., Idem, R., and Tontiwachwuthikul, P. (2016). Review on current advances, future challenges and consideration issues for post-combustion CO_2 capture using amine-based absorbents. Chin. J. Chem. Eng. 24: 278–288.

Lim, J., Kim, D., Yoon, Y., Jeong, S., Park, K., and Nam, S. (2012). Absorption of CO_2 into aqueous potassium salt solutions of alanine and proline. Energy Fuels 26: 3910–3918.

Lu, J., Fan, F., Liu, C., Zhang, H., Ji, Y., and Chen, M. (2011). Density, viscosity, and surface tension of aqueous solutions of potassium glycinate piperazine in the range of (288.15 to 323.15) K. J. Chem. Eng. Data 56: 2706–2709.

Ma, X. (2014). *Precipitation in carbon dioxide capture processes*, Ph.D. Thesis. Norway, Norwegian University of Science and Technology.

Mahmud, N., Benamor, A., Nasser, M., Al-Marri, M., Qiblawey, H., and Tontiwachwuthikul, P. (2017). Reaction kinetics of carbon dioxide with aqueous solutions of L-arginine, glycine & sarcosine using the stopped flow technique. Int. J. Greenh. Gas Con. 63: 47–58.

Majchrowicz, M., and Brilman, D. (2012). Solubility of CO_2 in aqueous potassium L-prolinate solutions-absorber conditions. Chem. Eng. Sci. 72: 35–44.

Majchrowicz, M., and Brilman, W. (2015). Amino acid salts for carbon dioxide capture: evaluating prolinate at desorber conditions. Energy Fuels 29: 3268–3275.

Majchrowicz, M., Brilman, D., and Groeneveld, M. (2009). Precipitation regime for selected amino acid salts for CO_2 capture from flue gases. Energy Procedia 1: 979–984.

Majchrowicz, M., Kersten, S., and Brilman, W. (2014a). Reactive absorption of carbon dioxide in prolinate salt solutions. Ind. Eng. Chem. Res. 53: 11460–11467.

Majchrowicz, M. (2014b). *Amino acid salt solutions for carbon dioxide capture*, Ph.D. Thesis. Netherlands, University of Twente.

Mazinani, S., Samsami, A., and Jahanmiri, A. (2011). Solubility, density, viscosity, and corrosion rate of carbon dioxide in blend solutions of monoethanolamine (MEA) and sodium glycinate (SG). J. Chem. Eng. Data 56: 3163–3168.

Mazinani, S., Ramazani, R., Samsami, A., Jahanmiri, A., and Van der Bruggen, B. (2015). Equilibrium solubility, density, viscosity and corrosion rate of carbon dioxide in potassium lysinate solution. Fluid Phase Equil. 396: 28–34.

Mock, B., Evans, L.B., and Chen, C.C. (1986). Thermodynamic representation of phase equilibria of mixed-solvent electrolyte systems. AIChE J. 32: 1655–1664.

Moioli, S., Pellegrini, L., Ho, M., and Wiley, D. (2019). A comparison between amino acid based solvent and traditional amine solvent processes for CO_2 removal. Chem. Eng. Res. Des. 146: 509–517.

Mondal, B., and Samanta, A. (2019). Equilibrium solubility and kinetics of CO2 absorption in hexamethylenediamine activated aqueous sodium glycinate solvent. Chem. Eng. J. 386: 121462.

Mondal, B., Bandyopadhyay, S., and Samanta, A. (2015). VLE of CO_2 in aqueous sodium glycinate solution-new data and modeling using Kent-Eisenberg model. Int. J. Greenh. Gas Con. 36: 153–160.

Murshid, G., and Butt, W. (2019). Investigation of thermophysical properties for aqueous blends of sarcosine with 1-(2-aminoethyl) piperazine and diethylenetriamine as solvents for CO_2 absorption. J. Mol. Liq. 278: 584–591.

Nwaoha, C., Supap, T., Idem, R., Saiwan, C., Tontiwachwuthikul, P., AL - Marri, M., and Benamor, A. (2017). Advancement and new perspectives of using formulated reactive amine blends for post-combustion carbon dioxide capture technologies. Petroleum 3: 10–36.

Park, S., Son, Y., Park, D., and Oh, K. (2008). Absorption of carbon dioxide into aqueous solution of sodium glycinate. Sep. Sci. Technol. 43: 3003–3019.

Park, S., Song, H., and Park, J. (2014). Selection of suitable aqueous potassium amino acid salts: CH_4 recovery in coal bed methane via CO_2 removal. Fuel Process. Technol. 120: 48–53.

Paul, S., and Thomsen, K. (2012). Kinetics of absorption of carbon dioxide into aqueous potassium salt of proline. Int. J. Greenh. Gas Con. 8: 169–179.

Perinu, C., Bernhardsen, I., and Knuutila, H. (2018). NMR speciation of aqueous MAPA, tertiary amines, and their blends in the presence of CO_2: influence of pKa and reaction mechanisms. Ind. Eng. Chem. Res. 57: 1337–1349.

Portugal, A., Magalhães, F., and Mendes, A. (2008). Carbon dioxide absorption kinetics in potassium threonate. Chem. Eng. Sci. 63: 3493–3503.

Portugal, A., Sousa, J., Magalhães, F., and Mendes, A. (2009). Solubility of carbon dioxide in aqueous solutions of amino acid salts. Chem. Eng. Sci. 64: 1993–2002.

Portugal, A., Derks, P., Versteeg, G., Magalhães, F., and Mendes, A. (2017). Characterization of potassium glycinate for carbon dioxide absorption purposes. Chem. Eng. Sci. 62: 6534–6547.

Rabensteiner, M., Kinger, G., Koller, M., Gronald, G., Unterberger, S., and Hochenauer, C. (2014). Investigation of the suitability of aqueous sodium glycinate as a solvent for post combustion carbon dioxide capture on the basis of pilot plant studies and screening methods. Int. J. Greenh. Gas Con. 29: 1–15.

Rabensteiner, M., Kinger, G., Koller, M., and Hochenauer, C. (2015). PCC pilot plant studies with aqueous potassium glycinate. Int. J. Greenh. Gas Con. 42: 562–570.

Ramazani, R., Samsami, A., Jahanmiri, A., and Mazinani, S. (2016). Characterization of monoethanolamine + potassium lysinate blend solution as a new chemical absorbent for CO_2 capture. Int. J. Greenh. Gas Con. 51: 29–35.

Ramezani, R., Mazinani, S., Di Felice, R., and Darvishmanesh, S. (2017a). Selection of blended absorbents for CO_2 capture from flue gas: CO_2 solubility, corrosion and absorption rate. Int. J. Greenh. Gas Con. 62: 61–68.

Ramezani, R., Mazinani, S., Di Felice, R., and Van der Bruggen, B. (2017b). Experimental and correlation study of corrosion rate, absorption rate and CO_2 loading capacity in five blend solutions as new absorbents for CO_2 capture. J. Nat. Gas Sci. Eng. 45: 599–608.

Ramezani, R., Mazinani, S., and Di Felice, R. (2018a). Potential of different additives to improve performance of potassium carbonate for CO_2 absorption. Korean J. Chem. Eng. 35: 2065–2077.

Ramezani, R., Mazinani, S., and Di Felice, R. (2018b). Characterization and kinetics of CO_2 absorption in potassium carbonate solution promoted by 2-methylpiperazine. J. Environ. Chem. Eng. 6: 3262–3272.

Ramezani, R., Mazinani, S., and Di Felice, R. (2019). A comprehensive kinetic and thermodynamic study of CO_2 absorption in blends of monoethanolamine and potassium lysinate: experimental and modeling. Chem. Eng. Sci. 206: 187–202.

Salazar, V., Sanchez-Vincente, Y., Pando, C., and Renuncio, J. (2010). Enthalpies of absorption of carbon dioxide in aqueous sodium glycinate solutions at temperatures of (313.15 and 323.15) K. J. Chem. Eng. Data 55: 1215–1218.

Sanchez-Fernandez, E., Heffernan, K., Ham, L., Linders, M., Eggink, E., Schrama, F., Brilman, D., and Goetheer, E. (2013b). Conceptual design of a novel CO_2 capture process based on precipitating amino acid solvents. Ind. Eng. Chem. Res. 52: 12223–12235.

Sanchez-Fernandez, E., Heffernan, K., Ham, L., Linders, M., Brilman, D., and Goetheer, E. (2014). Analysis of process configurations for CO_2 capture by precipitating amino acid solvents. Ind. Eng. Chem. Res. 53: 2348–2361.

Sanchez-Fernandez, E. (2013a). *Novel process designs to improve the efficiency of post combustion carbon dioxide capture*, Ph.D. Thesis. Delft, The Netherlands, Delft University of Technology.

Sefidi, V.S. and Luis, P. (2019). Advanced amino acid based technologies for CO_2 capture: a review. Ind. Eng. Chem. Res. 58: 20181–20194.

Shaikh, M., Shariff, A., Bustam, M., and Murshid, G. (2013). Physical properties of aqueous blends of sodium glycinate (SG) and piperazine (PZ) as a solvent for CO_2 capture. J. Chem. Eng. Data 58: 634–638.

Shaikh, M., Shariff, A., Bustam, A., and Murshid, G. (2014). Physicochemical properties of aqueous solutions of sodium prolinate as an absorbent for CO_2 removal. J. Chem. Eng. Data 59: 362–368.

Shaikh, M., Shariff, A., Bustam, M., and Murshid, G. (2015a). Measurement and prediction of physical properties of aqueous sodium l-prolinate and piperazine as a solvent blend for CO_2 removal. Chem. Eng. Res. Des. 102: 378–388.

Shaikh, M., Shariff, A., Bustam, M., and Murshid, G. (2015b). Physicochemical properties of aqueous solutions of sodium glycinate in the non-precipitation regime from 298.15 to 343.15 K. Chin. J. Chem. Eng. 23: 536–540.

Shaikh, M., Shariff, A., Garg, S., and Bustam, M. (2017). Physical properties of aqueous solutions of potassium L-prolinate from 298.15 to 343.15 K at atmospheric pressure. Chem. Pap. 71: 1185–1194.

Shariff, A.M. and Shaikh, M.S. (2017). Aqueous amino acid salts and their blends as efficient absorbents for CO_2 capture. In: Budzianowski, W. (Ed.). *Energy efficient solvents for CO_2 capture by Gas-Liquid absorption. Green energy and technology*. Springer, Cham. https://doi.org/10.1007/978-3-319-47262-1_6.

Shen, S., and Yang, Y. (2016a). Carbon dioxide absorption into aqueous potassium salt solutions of arginine for post-combustion capture. Energy Fuels 30: 6585–6596.

Shen, S., Feng, X., and Ren, S. (2013a). Effect of arginine on carbon dioxide capture by potassium carbonate solution. Energy Fuels 27: 6010–6016.

Shen, S., Feng, X., Zhao, R., Ghosh, U., and Chen, A. (2013b). Kinetic study of carbon dioxide absorption with aqueous potassium carbonate promoted by arginine Chem. Eng. J. 222: 478–487.

Shen, S., Yang, Y., Wang, Y., Ren, S., Han, J., and Chen, A. (2015). CO_2 absorption into aqueous potassium salts of lysine and proline: density, viscosity and solubility of CO_2. Fluid Phase Equil. 399: 40–49.

Shen, S., Yang, Y., Zhao, Y., and Bian, Y. (2016b). Reaction kinetics of carbon dioxide absorption into aqueous potassium salt of histidine. Chem. Eng. Sci. 146: 76–87.

Shen, S., Yang, Y., Bian, Y., and Zhao, Y. (2016c). Kinetics of CO_2 absorption into aqueous basic amino acid salt: potassium salt of lysine solution. Environ. Sci. Technol. 50: 2054–2063.

Shen, S., Zhao, Y., Bian, Y., Wang, Y., Guo, H., and Li, H. (2017a). CO_2 absorption using aqueous potassium lysinate solutions: vapor-liquid equilibrium data and modelling. J. Chem. Thermodyn. 115: 209–220.

Shen, S., Bian, Y., and Zhao, Y. (2017b). Energy-efficient CO_2 capture using potassium prolinate/ethanol solution as a phase-changing absorbent. Int. J. Greenh. Gas Con. 56: 1–11.

Simons, K., Brilman, W., Mengers, H., and Nijmeijer, K. (2010). Kinetics of CO_2 absorption in aqueous sarcosine salt solutions: influence of concentration, temperature, and CO_2 loading. Ind. Eng. Chem. Res. 49: 9693–9702.

Sodiq, A., Rayer, A., Olanrewaju, A., and Zhra, M. (2014). Reaction kinetics of carbon dioxide (CO_2) absorption in sodium salts of taurine and proline using a stopped-flow technique. Int. J. Chem. Kinet. 46: 730–745.

Song, H., Lee, S., Maken, S., Park, J., and Park, J. (2006). Solubilities of carbon dioxide in aqueous solutions of sodium glycinate. Fluid Phase Equil. 246: 1–5.

Song, H., Lee, M., Kim, H., Gaur, A., and Park, J. (2011). Density, viscosity, heat capacity, surface tension, and solubility of CO_2 in aqueous solutions of potassium serinate. J. Chem. Eng. Data 56: 1371–1377.

Song, H., Park, S., Kim, H., Gaur, A., Park, J., and Lee, S. (2012). Carbon dioxide absorption characteristics of aqueous amino acid salt solutions. Int. J. Greenh. Gas Con. 11: 64–72.

Sreedhar, I., Nahar, T., Venugopal, A., and Srinivas, B. (2017). Carbon capture by absorption-path covered and ahead renewable and sustainable. Energy Rev. 76: 1080–1107.

Suleman, H., Maulud, A., and Syalsabila, A. (2018). Thermodynamic modelling of carbon dioxide solubility in aqueous amino acid salt solutions and their blends with alkanolamines. J. CO_2 Util. 26: 336–349.

Svendsen, H., Hessen, E., and Mejdell, T. (2011). Carbon dioxide capture by absorption, challenges and possibilities. Chem. Eng. J. 171: 718–724.

Syalsabila, A., Shah Maulud, A., Suleman, H., and Nordin, N. (2019). VLE of carbon dioxide-loaded aqueous potassium salt of histidine solutions as a green solvent for carbon dioxide capture: experimental data and modelling. Int. J. Chem. Eng. 2019: 1–11.

Talkhan, A., Benamor, A., Nasser, M., Qiblawey, H., El-Tayeb, S., and Marsafy, S. (2019). Corrosion study of carbon steel in CO_2 loaded solution of methyldiethanolamine and L-arginine mixtures. J. Electroanal. Chem. 837: 10–21.

Thee, H., Nicholas, N., Smith, K., and da Silva, G. (2014). A kinetic study of CO_2 capture with potassium carbonate solutions promoted with various amino acids: glycine, sarcosine, and proline. Int. J. Greenh. Gas Con. 20: 212–222.

Wei, C., Puxty, G., and Feron, P. (2014). Amino acid salts for CO_2 capture at flue gas temperatures. Chem. Eng. Sci. 107: 218–226.

Xiang, Q., Fang, M., Yu, H., and Maeder, M. (2012). Kinetics of the reversible reaction of CO_2 and HCO_3^- with sarcosine salt in aqueous solution. J. Phys. Chem. A 116: 10276–10284.

Xiang, Q., Fang, M., Maeder, M., and Yu, H. (2013). Effect of sarcosinate on the absorption kinetics of CO_2 into aqueous ammonia solution. Ind. Eng. Chem. Res. 52: 6382–6389.

Yan, S., He, Q., Zhao, S., Zhai, H., Cao, M., and Ai, P. (2015). CO_2 removal from biogas by using green amino acid salts: performance evaluation. Fuel Process. Technol. 129: 203–212.

Yang, N., Xu, D., Wei, C., Puxty, G., Yu, H., Maeder, M., and Norman, S. (2014a). Protonation constants and thermodynamic properties of amino acid salts for CO_2 capture at high temperatures. Ind. Eng. Chem. Res. 53: 12848–12855.

Yang, N., Xu, D., Yu, H., Conway, W., Maeder, M., and Feron, P. (2014b). Potassium sarcosinate promoted aqueous ammonia solution for post-combustion capture of CO_2. Greenh. Gas Sci. Technol. 4: 555–567.

Ying, J., and Eimer, D. (2013). Determination and measurements of mass transfer kinetics of CO_2 in concentrated aqueous monoethanolamine solutions by a stirred cell. Ind. Eng. Chem. Res. 52: 2548–2559.

Yoo, Y., Kang, D., Kim, I., and Park, J. (2018). Investigation of thermodynamic properties on CO_2 absorbents blended with ammonia, amino acids, and corrosion inhibitors at 313.15–353.15 K. J. Chem. Eng. Data 63: 2856–2867.

Yu, B., Yu, H., Li, K., Yang, Q., Zhang, R., Li, L., and Chen, Z. (2017). Characterisation and kinetic study of carbon dioxide absorption by an aqueous diamine solution. Appl. Energy 208: 1308–1317.

Zarogiannis, T., Papadopoulos, A., and Seferlis, P. (2016). Systematic selection of amine mixtures as post-combustion CO_2 capture solvent candidates. J. Clean. Prod. 136: 159–175.

Zhang, Z., Li, Y., Zhang, W., Wang, J., Soltanian, M., and Ghani, A. (2018). Effectiveness of amino acid salt solutions in capturing CO_2: a review. Renew. Sust. Energ. Rev. 98: 179–188.

Zhao, Y., Shen, S., Bian, Y., Yang, Y., and Ghosh, U. (2017a). CO_2 solubility in aqueous potassium lysinate solutions at absorber conditions. J. Chem. Thermodyn. 111: 100–105.

Zhao, Y., Bian, Y., Li, H., Guo, H., Shen, S., Han, J., and Guo, D. (2017b). A comparative study of aqueous potassium lysinate and aqueous monoethanolamine for post-combustion CO_2 capture. Energy Fuels 31: 14033–14044.